MATERIALS CHEMISTRY FRONTIERS

CCS 中国化学会 CHINESE CHEMICAL SOCIETY

ICCAS

ROYAL SOCIETY OF CHEMISTRY

REVIEW

View Article Online
View Journal | View Issue

Cite this: *Mater. Chem. Front.*, 2024, **8**, 1703

Applications of amorphous inorganics as novel functional materials

Zhengxi Guo, Zhaoming Liu* and Ruikang Tang *

Received 1st December 2023,
Accepted 10th January 2024

DOI: 10.1039/d3qm01263h

rsc.li/frontiers-materials

Amorphous inorganics have attracted much attention because of their long-range disordered structure with advantageous functional properties. In this minireview, novel advances in amorphous inorganics (*e.g.*, metal, metallic oxide, and metallic salts) and their preparation strategies are highlighted and summarized. The intrinsic atomic structure of amorphous materials in short-, medium-, and long-range orientations is discussed. The relationships between their structural features (*e.g.*, disorderliness, defects, metastability, isotropy, and flexible structure) and related properties are demonstrated. Their current characterization techniques for amorphous structures are presented as well. The applications of these amorphous inorganics are illustrated, covering the fields of mechanical, electrical, biomedical, and catalytical materials. Finally, future challenges and perspectives in the field of amorphous inorganics are discussed, and this review emphasizes the unique and important role of amorphous inorganics in the development of more advanced materials.

1. Introduction

Inorganic materials have played a dominant role in functional material utilization, driving the ongoing pursuit of novel advancements.[1] Among them, the emergence of amorphous inorganics, also known as non-crystalline inorganics, has attracted much attention owing to their distinctive properties and capabilities.[2–4] The discovery of amorphous inorganic materials traces back to ancient times when humans encountered naturally occurring glass.[5] However, it was only in the early 20th century that scientists began to truly understand the unique nature of amorphous inorganics and embarked on systematic investigations.[6] Up to now, amorphous inorganics have impacted numerous aspects of modern society, and they are utilized in a broad range of applications such as glass,[7–12] electrodes,[13–16] conductors,[17–19] biomaterials,[20–22] and catalysts.[23–26] The development of advanced synthesis techniques and the increasing demand for customizable material properties have further propelled the exploration and utilization of fascinating amorphous inorganics.

In amorphous inorganics, metals,[27–29] metallic oxides,[30–32] and metallic salts[33–35] are the major components, representatively serving as functional materials for application. For example, amorphous metals, also known as amorphous alloys or metallic glass, are a kind of mechanical materials, favouring highly strengthened mechanical performance.[36] Additionally, amorphous metallic oxides are promising

Department of Chemistry, Zhejiang University, Hangzhou, Zhejiang 310027, People's Republic of China. E-mail: oldliu@zju.edu.cn, rtang@zju.edu.cn

Zhengxi Guo

Zhengxi Guo received his degrees (BSc in 2016 and MSc in 2020) from Guangxi Normal University. He is currently pursuing his PhD in the Department of Chemistry at Zhejiang University. His research interests focus on the fabrication of functional amorphous materials via inorganic ionic polymerization.

Zhaoming Liu

Prof. Zhaoming Liu received his BSc and PhD degrees at the Department of Chemistry, Zhejiang University in 2013 and 2017. He is currently a professor in the Department of Chemistry at Zhejiang University. His research focuses on crystal growth, inorganic ionic polymerization, biomineralization and biomimetic materials.

new-type semiconductors, benefiting from electrochemical conversion.[37] Moreover, amorphous metallic salts such as amorphous calcium carbonate (ACC) and amorphous calcium phosphate (ACP) fundamentally support the growth of biological skeleton.[38] It is noteworthy that the importance of these amorphous inorganics needs to be briefly and systematically illustrated from species to application. In other words, their functional performances rely on ingenious regulations of atoms, indicating a significant relationship between the structures and properties of amorphous inorganics.

The structures and properties of amorphous inorganics are vastly distinct from crystalline inorganics owing to their long-range atomic disordering.[39] Disordered atomic structures expose more coordinating defects of amorphous inorganics, endowing the materials with various properties in a broad functional range.[40]

For instance, amorphous metallic glasses are greatly enhanced in terms of ductility and strength owing to their atomic dislocation motion.[41] Coordinatively unsaturated sites and interfacial defects endow amorphous inorganics with great potential in catalytical and electrochemical reactive devices.[42] Moreover, the large specific surface area,[43] facilely modifiable mobility,[44] bio-accessibility,[45] and fluidity[46] of amorphous inorganic nanomaterials have promisingly provided candidates for drug delivery, therapeutics, diagnostics, hard-tissue repairs, and other biomedical utilizations. Thus, insights into the relationship between structures and properties are significant for the rational design of amorphous inorganics, making them key factors in their functional utilization.

In this minireview, we briefly introduce amorphous inorganics in their representative applications and focus on their correlation between non-crystalline atomic structures and advanced properties. In addition, some future perspectives on amorphous inorganics among different applied fields are provided. The major contents of this minireview are schematically demonstrated in Fig. 1. We expect that this minireview can provide a deep cognation into amorphous inorganics and emphasize the significant contribution of functional material research, as well as their potential in the development of future functional material.

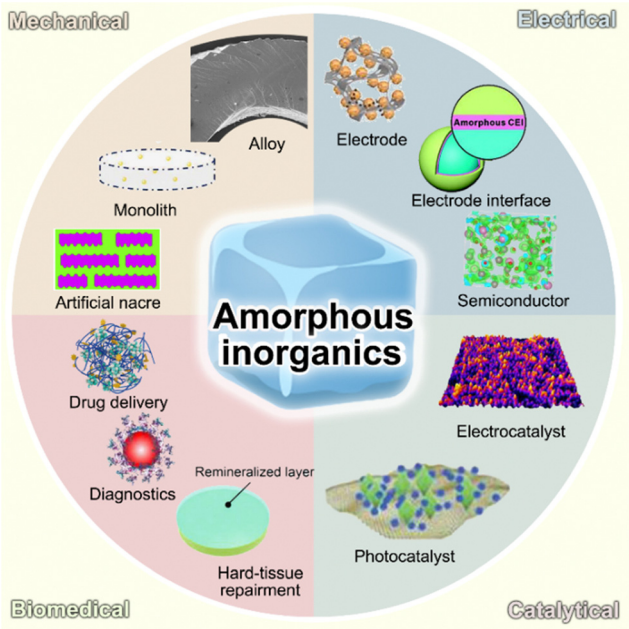

Fig. 1 Schematic illustration of representative amorphous inorganics and their utilization for mechanical, electrical, biomedical, and catalytic applications.

Ruikang Tang

Prof. Ruikang Tang studied chemistry at Nanjing University and completed his PhD in 1998. Subsequently, he worked at the State University of New York at Buffalo as a postdoctoral research fellow and research assistant professor. He is currently a professor in the Department of Chemistry, Zhejiang University and the State Key Laboratory of Silicon Materials. In 2006, he established the Center for Biomaterials and Biopathways and became a Changjiang Scholar Chair Professor of the Ministry of Education of China. His research focuses on biomineralization, biomaterials and biomimetic pathways.

2. Amorphous structure and its functional relationship

Amorphous inorganic refers to a broad range of inorganic materials that lack a long-range order in their atomic arrangement. The atomic structure of amorphous inorganics is characterized by a random arrangement of atoms, with no distinct crystalline lattice or periodic pattern. Compared with their crystalline counterparts, this disordered arrangement gives amorphous inorganics unique properties. For instance, amorphous inorganics tend to be isotropic, meaning that they have similar properties in all directions, whereas crystalline structures exhibit anisotropic behaviours, leading to variations in their properties depending on the crystallographic direction. In this section, the cognations of amorphous structures are described, and an understanding of their unique properties is introduced.

2.1 Atomic structure

A crystalline state is regularly formed from unit cells within a translational symmetry feature, proceeding in a long-range order. On the contrary, the metastable amorphous state is randomly disordered in a long-range distance. In contrast, an amorphous state has proceeded orderliness in the short- and medium-range, which are dominant features to describe the

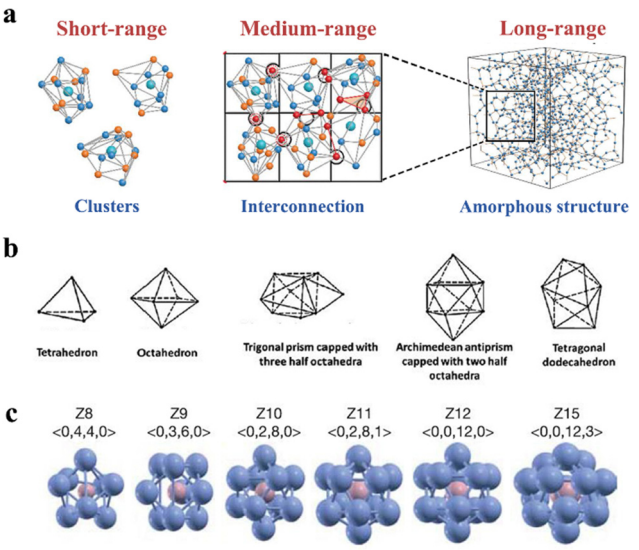

Fig. 2 (a) Schematic illustration of atoms distributed in the short-, medium-, and large-range. Copyright 2022, The Royal Society of Chemistry.[27] (b) Five basic Bernal polyhedrals that describe atomic distribution in the short range. Copyright 1983, American Physical Society.[47] (c) Kasper polyhedron of multi-atomic component of short-range clusters and their symmetry. Copyright 2006, Springer Nature.[48]

structure.[47,48] Knowledge of orderliness in the amorphous structure is the key to recognizing its instinct features, thus designing more candidates for functional materials. In this section, the orderliness of amorphous inorganics is introduced as a fellow, covering the short-, medium-, and long-range (Fig. 2a).

2.1.1 Short-range order (SRO). Short-range is the scale of a fundamental structure in a lattice, typically consisting of one or two atom spacings, approximately ranging within 5 Å.[49]

Atoms usually consist of regular bindings and predicable units, performing an ordering atomic combination on this scale. Theoretically, several structural models have been proposed to describe the characteristics of amorphous structures, including the dense random packing model, the solute-centred cluster model, and the polytetrahedral packing model. These models aim to uncover the atomic locations within the structures.

The dense random packing model has been widely accepted in the field of materials science, as it provides a simple and effective way to describe the arrangement of atoms and molecules in liquids and solids.[48,50] This model was proposed by Bernal to describe the SRO, as they can be counted and analysed using computer simulations and experimental techniques, such as X-ray diffraction. Descriptions in the SRO of Bernal's model involve five basic Bernal polyhedrals (Fig. 2b), as they predominantly combine with tetrahedra.[47] However, the existing model has its limitations because it assumes that all atoms have the same hard spheres, making it unsuitable for representing systems with varying component sizes. To address this issue, solute-centred clusters are proposed, which have been validated by both theoretical and experimental findings.[51]

According to the solute-centred cluster model, clusters that feature solute atoms occupying the spaces left by the solvent atoms form the foundation of amorphous structures. Voronoi polyhedron is commonly utilized to characterize these clusters, where the planar faces cut perpendicularly through the lines connecting an atom to its neighbouring atoms.[52] Despite the numerous descriptions of polyhedron types, Kasper polyhedra describes that the distinction of disclination involves the minimum number of atoms. In Fig. 2c, the polyhedrons illustrate the distinction of atomic packing configurations in various Kasper modes.[48]

The coordination number, also known as the type of polyhedron, is a critical factor in describing the effective size ratio between the solute and solvent atoms.[53,54] Altering the composition of amorphous materials can lead to a change in the type of cluster, which ultimately affects the atomic structure and properties. Researchers, such as Cheng and colleagues, have found that adding Al atoms into $Cu_{46}Zr_{54}$ can significantly increase the prevalence of $\langle 0,0,12,0\rangle$ icosahedra clusters.[55] Icosahedral clusters are ordered with five-fold symmetry, which is stable and highly favoured in short-range order. Because an icosahedral order is also a defining feature of quasicrystals, there could be structural similarities between quasicrystals and amorphous structures that merit further investigation. In addition to the structural order, chemical orders are also present in the short-range order of amorphous structures, indicating a preference for certain elemental connections.

2.1.2 Medium-range order (MRO). Observably, the orderliness arrangement exhibits a degree of organization surpassing the short-range order in the vicinity of 5–20 Å, which is referred to as the medium-range order.[56] In nucleation, the solute-cantered clusters pack efficiently by sharing solvent atoms in the shell, which constitutes the MRO of the amorphous structure. Additionally, variations in the MRO can lead to alterations in the atomic structure and retain the structural stability of amorphous nanomaterials.[57] For instance, Lan and colleagues discovered that amorphous Pd–Ni–P metallic glass nanoparticles (MGNP) performed an MRO rearrangement against harmful crystallization during long-term CV cycles.[58] The MGNP could transform between two- to three-atom modes at MRO, plays a crucial role in stabilizing its amorphous state and prevents crystalline-induced degradation.

Moreover, Cherevko's research group investigated the distinction in the medium-range linking type of the [IrO_6] octahedron between crystalline and amorphous forms of IrO_2.[59] This investigation was carried out during the leaching process of non-noble elements in mixed iridium-based perovskites. In the amorphous IrO_2, the medium local structure engenders a random connection configuration, making activated oxygen sites increase with a low coordination number. This intriguing relationship between MRO and the catalytic performance of amorphous nanocatalysts offers an alternative path for manipulating their catalytic properties.

2.1.3 Long-range disorder. The long-range atomic scale of amorphous structure refers to the overall arrangement of atoms in the material. In crystalline material, the arrangement of

atoms is uniform as it periodically extends over long-range distances. Unlike crystals, amorphous materials do not have a well-defined long-range structure, meaning they have a random and disordered arrangement of atoms, which is characterized as a long-range disorder.[60] In amorphous inorganic materials, the presence of a long-range disorder can significantly influence mechanical strength, conductivity, and electrical conductivity. Thus, the understanding of amorphous inorganics between their disorder structure and unique properties is crucial for novel insight into future material design.

2.2 Structure–property–function relationships

Obviously, an understanding of the relationship between amorphous structure and function is significant for developing advanced functional materials. Specifically, the functional performances are directly related to these features (*e.g.*, disorderliness, defect, isotropy, metastability, and flexible structure) of an amorphous structure, and they are structurally distinct from a crystalline structure. To address this, we briefly summarize these specific features (Fig. 3a–e) and highlight their contribution to functional regulation.

2.2.1 Disorderliness. Compared with crystals, long-range disorderliness is the typical feature of amorphous structure. It correlates with distinct properties with behaviours differently from crystals in the bulk phase. For example, disorderliness breaks the long-range translational lattice symmetry in inorganics, and it affects the mechanical properties with the unique performance of amorphous materials (Fig. 3a).[61] In amorphous

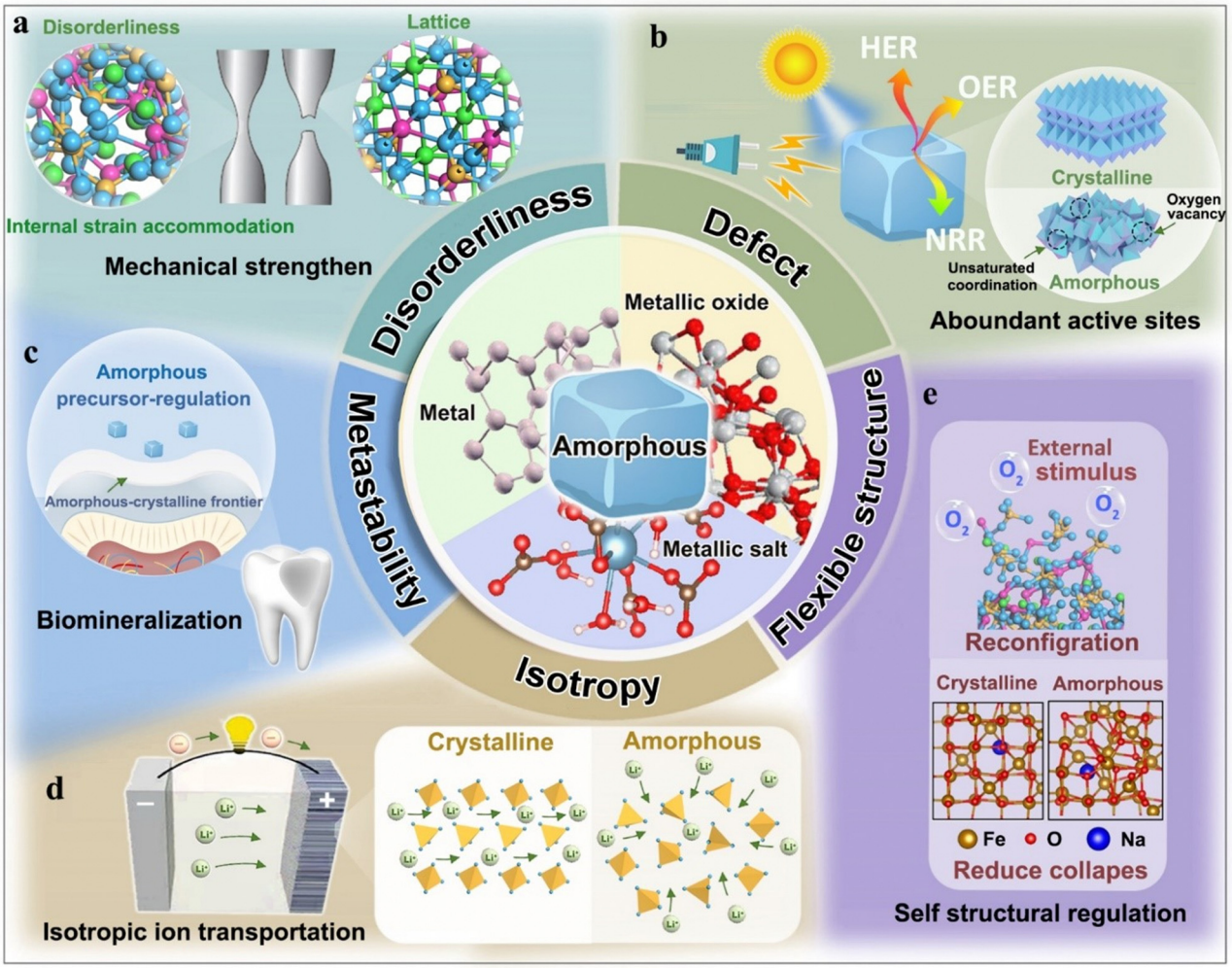

Fig. 3 Schematic illustration of representative features in amorphous inorganics; core inset: atomic structural examples include metal (Ni_3Nb_7), metallic oxide (TiO_2), and metallic salts ($CaCO_3$). (a) Disorderliness (in amorphous structure, atom arrangement is disordered; meanwhile, it accommodates internal strain, introducing distinct mechanical behaviour compared with corresponding crystalline counterparts.). (b) Defects (amorphous structure internally consists of numerous active sites that far exceed what is in the crystalline structure, benefiting from enhanced catalysis reactions, such as the hydrogen evolution reaction (HER), oxygen evolution reaction (OER), and nitrogen reduction reaction (NRR)). (c) Metastability (amorphous precursor is facile to regulate biomineralization, performing adjustable metastability for biomedical utilization, such as hard tissue repair). (d) Isotropy (amorphous structure) is homogeneous, indicating an isotropic Li^+ diffusion, whereas crystalline structure is anisotropic, performing directional Li^+ emigrations. (e) Flexible structure (amorphous material has a flexible structure that is self-regulatable at the atomic scale under various applied conditions, such as catalysis and ion conduction).

alloys, the mechanical is distinct from the crystals, performing superior behaviours. This is because the broken symmetry changes atomistic deformation, meaning that the internal strain can be readily accommodated through atomic rearrangement in the neighborhood.[62] Guo and colleagues developed an artificial tooth enamel (ATE) through the regulation of the amorphous intergranular phase. In the preparation of ATE, the as-prepared amorphous ZrO_2-coated hydroxyapatite can be assembled into a continuously dense structure on the molecular scale, persuading an ingenious regulating strategy of amorphous intergranular phase into high-performed inorganic material preparation.[63] In ionic conduction, long-range disorderliness shortens the distance of ion transportation, and it decreases the bond dissociation energy, which promotes their ion diffusion kinetics.[64] Moreover, the presence of unsaturated coordination in amorphous oxides highlights the inherent disorder and lack of long-range order in their atomic arrangement. It is crucial to tailor the catalytical property through the energy gap hanging of amorphous oxide materials. For example, unsaturated Bi–O coordination led amorphous BiO_x to display distinct Bi^{2+} and Bi^{+} oxidation states, performing a selective p-orbital catalytic activity for the nitrogen reduction reaction.[65]

2.2.2 Defect. A defect is a typical feature of amorphous inorganics (Fig. 3b) commonly raised by disorder structures.[66] There are abundant defects that occur in the skeleton of the disorderliness structure, originating during its amorphization. Owing to their vast quantities and activities, these defects (*e.g.*, oxygen vacancies and unsaturated coordination) lead to high chemical reactivities, such as catalysis and ion storage.[67–74] Oxygen vacancy is one type of well-known defect in crystalline engineering due to the absence of oxygen atoms at their lattice positions. In amorphous materials, the quantity of oxygen vacancies is far more than that in crystals, performing distinctly enhanced functions, especially in catalysis.[65–70] Additionally, the design of amorphous electrodes with a combination of oxygen vacancy and disordered structure was capable of enhanced ion storage. In alkali metal ion batteries, storages of Na^+ and K^+ in electrodes were restricted by lattice owing to their relatively large atomic radius. However, the vacancy in the amorphous phase was demonstrated to enhance the ion storage performance, such as Li^+, Na^+ and K^+.[71–73] In addition to reactive activity, electron transfer properties, such as surface-enhanced Raman scattering (SERS), of amorphous inorganics are unique to their corresponding crystalline compounds. Owing to its low coordination number and plentiful oxygen defects, amorphous ZnO exhibited a higher electronic density of states and a narrower energy gap.[74] Consequently, it demonstrated an enhanced SERS activity compared to its crystalline counterparts.

2.2.3 Metastability. Amorphous inorganics, especially their precursors, perform metastability. This metastable state allows amorphous precursors to be capable of controlling the nucleation and growth of minerals.[75] In biomineralization, the regulation of amorphous precursors plays a significant role in the formation of amorphous-crystalline mineralized frontiers in living organisms (Fig. 3c).[76] These amorphous precursors can also be utilized for artificial design to construct highly mineralized biomaterials as inorganic amorphous constituents.[77] Moreover, metastability makes amorphous inorganics facile to regulate the repair and regeneration of biominerals. In addition, an amorphous structure instinctually preserves a high specific surficial area and porous skeleton for effective drug delivery.[78] Meanwhile, the metastable amorphous structure is a favourite for dissolution, facilitating its controllable drug release.[79,80]

2.2.4 Isotropy. Amorphous inorganics tend to be isotropic, meaning that they have similar structures and properties in all directions, whereas crystalline structures exhibit anisotropy. In optical materials, isotropic amorphization is favoured in the preparation of transparent glass because it essentially overcomes birefringence, which is caused by an anisotropic structure such as a lattice.[81] In electrochemical reactions, the disorderliness of atomic arrangement changes pathways in ion diffusion and storage.[82] In the well-known cathode material (*e.g.*, $LiCoO_2$ and $LiFePO_4$), while the atomic structure turns from crystalline grain to amorphous phase, the immigrated path of Li^+ ions changes from 2D-layer and 1D-channel intercalation to 3D diffusion, contributing a fast isotropic ion transportation and a pseudocapacitive behaviour.[83]

2.2.5 Flexible structure. Flexible structure is another important advance feature of amorphous material. At the atomic scale, the flexible structure can self-regulate, leading to materials that improve its performance against external stimuli under various applied conditions, such as catalysis and ion conduction (Fig. 3e). For example, amorphous NiFeMo oxide has superior performance in catalysing the oxygen evolution reaction (OER) owing to its fast surface reconstruction. This development is significant for amorphous metal oxides, as they can rapidly reconstruct their surfaces and reform the active layer rich in oxygen vacancies, whereas this process is sluggish for the crystalline counterpart.[84] Furthermore, amorphous Co hydroxide is one kind of OER catalyst that can reconfigure and optimize its spatial coordination structure to adapt to external stimuli that catalyze oxygen evolution.[85] Thus, it overcame the structural restrictions in the stiff lattice, performing highly stable and effective OER catalysis. Additionally, in amorphous ion-conductors, atomic-scale flexibility made them ingeniously overcome the exact ''collapse'' of the crystalline structure.[86,87] This is because the amorphous structure mitigated the structural volume changes during the insertion or extraction of ions. Compared with crystalline counterparts, amorphous Fe_2O_3 performs much lower insert energy, and it geometrically displays negligible volume change after Na^+ insertion.[88] It also fits with ionic compounds, such as $NaFePO_4$, in which the amorphous structure lowers barriers during Na migration.[89]

3. Representative amorphous inorganics and formation mechanisms

The spices of amorphous inorganics are numerous, including metal, metallic oxide, and metallic salt.[27–35] Their long-range

disordering atomic structures are specific features compared with their crystalline counterparts. These materials are receiving much attention, especially in their formation mechanism. In this respect, we briefly introduce representative amorphous inorganics and their formation mechanism.

3.1 Representative amorphous inorganics

Metals, metallic oxides, and metallic salts are the most representative species of amorphous inorganic materials, and they play vital roles in many applications, including mechanical, biomedical, electrical, and catalytic materials. Each as-mentioned aspect is illustrated as follows. Moreover, other amorphous inorganic species, such as metallic sulphides, metallic phosphides, and non-metallic inorganics (*e.g.*, amorphous carbon-based and amorphous silicon-based inorganics), are introduced in this section as well.

3.1.1 Amorphous metal. Amorphous metal is known as metallic glass, forming a long-range disordered atomic structure.[90] The chemical composition of amorphous metallic materials is a multi-component system. Amorphous metals are made by rapidly cooling a liquid metal to form a solid that has no internal structure or crystalline order.[91] This unique characteristic gives amorphous metallic materials various properties, such as high strength, corrosion resistance, and electrical properties.[92] The pioneer research of amorphous alloys was presented by Duwez and co-workers in 1960, who accidentally discovered a solid solution consisting of two elements from totally different lattice structures and valences.[93] Afterwards, numerous amorphous alloys have been prepared and widely utilized in various applications.

3.1.2 Amorphous metallic oxides. Amorphous metallic oxides are another species of amorphous inorganics that also cover amorphous ceramics, such as amorphous ZrO_2, Al_2O_3, and Y_2O_3.[94–96] These amorphous materials are made by combining metal elements with oxygens, foaming in a solid material that has a disordered structure. Owing to their unique structure, amorphous metallic oxides have a wide range of applications, including as catalysts for chemical reactions, semiconductors for chip utilization, and as components in electrodes.[97] Amorphous $InGaZnO_4$ (a-IGZO), the most famous semiconductive material, is a transistor channel material that demonstrates the success of non-crystalline oxides.[98] A-IGZO is initially applied in thin-film-transistor display backplanes, and it has been utilized as a transistor channel material for static random-access memory and has served as a memory selector in dynamic random access memory devices.[99] Besides, amorphous metallic oxides can also serve as a catalyst for the reaction of chemicals, such as hydrogen evolution reaction and oxygen evolution reaction.[27] By incorporating amorphous metallic oxides into catalysts, their unsaturated metal atoms can promote the catalytical reaction compared with their crystalline counterparts.[27] Additionally, amorphous metallic oxides have been explored as high energy density materials for use in batteries, as they offer high charge and discharge rates and low internal resistance.[31]

3.1.3 Amorphous metallic salts. Amorphous metallic salts are another type of amorphous inorganics that has unique properties. These materials are created by combining metal cations and non-metallic anions, resulting in a material that has a disordered structure. Amorphous metallic salts have been applied in various areas, including the development of high-performed mechanical materials.[100] One of the representatives of amorphous metallic salts is in the development of rechargeable lithium-ion batteries, where they can deeply understand the structural and functional differences between amorphous and corresponding crystalline parts, such as a decrease in open circuit voltage in amorphization.[101] Additionally, amorphous metallic salts, such as amorphous calcium carbonate and amorphous calcium phosphate, have been incorporated into biomaterials, which have the potential for bio-repairment and bio-regeneration.[102]

3.1.4 Amorphous metallic phosphides. Metal phosphides differ from other metallic salts owing to their high conductivity and significant catalytic activity when interacting with P and metal atoms.[103] Amorphous metal phosphide is a type of metal phosphide that has a metastable nature, exhibiting short-/medium-range ordered and long-range disordered structures. This unique structure enables the material to have more active sites and a more suitable electronic structure for electrocatalysis compared to its crystalline counterparts.[104] Researchers have extensively studied subgroup elements, such as Co, Ni, Mo, W, and Ru, to fabricate amorphous metallic phosphide electrocatalysts.[105]

3.1.5 Amorphous metallic sulphides. Unlike their crystalline counterpart, amorphous metallic sulphides exhibit long-range disordered and short-range ordered atomic arrangements, which can lead to lattice distortion and unsaturated bonds. These structures contribute to their high reactivity and flexibility, demonstrating an enhanced catalytic performance.[106] Currently, several amorphous metallic sulphides have been studied, such as amorphous MoS, amorphous CdS, and amorphous CoS.[107] For example, the active sites of crystalline MoS mainly exist at the edges, whereas the atomic structure of a-MoS imparted numerous active sites owing to its instinct disorder structure.[108] In the structure of a-MoS, $[Mo_3S_{13}]^{2-}$ clusters or $[MoS_6]^{-}$ units exist as the fundamental cores in the short-range; meanwhile, their long-range disorderliness exposes more active sites, benefiting from catalytical performance.

3.1.6 Amorphous carbon-based inorganics. In contrast to graphite and graphene, amorphous carbon-based inorganics do not possess regular lattice structures, whereas they have disordered structures with a lack of long-range periodicity.[109] Carbon-based amorphous materials comprise various forms, including amorphous hard carbon and soft carbon.[110] These materials exhibit unique electrical and chemical properties, making them useful in battery electrodes. In recent years, there has been renewed interest in amorphous carbons, particularly hard carbon, owing to their extraordinary performance in sodium insertion.[111] This is attributed to their expanded layered structures compared to graphite, as well as their

disordered features. Along with the presence of micro domains and a lower degree of graphitization, these characteristics enable the relatively large sodium ions to be easily intercalated, resulting in significantly higher specific capacities compared to graphite.

3.1.7 Amorphous silicon-based inorganics. Silicon-based amorphous non-metallic inorganics refer to non-crystalline forms of silicon, including amorphous silicon (a-Si),[112] silicon dioxide,[113] and silicon carbide (a-SiC).[114] Amorphous silicon is commonly used in thin-film solar cells and photovoltaic devices, as it efficiently converts sunlight into electricity.[112] Amorphous silicon dioxide, also known as amorphous silica, is highly valued for its exceptional thermal stability, high melting point, and insulating properties.[113] It has wide application in glass manufacturing, electronics, ceramics, catalyst supports, and as a filler in various materials. A-SiC is a compound of silicon and carbon and has been distinguished by its high strength and superior chemical stability.[114]

3.2 Formation mechanism

In natural biominerals, the biological regulation of the amorphous precursors and intermediates is significant in the formation of mechanical materials.[115,116] In the laboratory, there are numerous strategies used to prepare inorganic amorphous structures, such as nucleation (Fig. 4a),[117] liquid–liquid phase separation (Fig. 4b),[118] and inorganic ionic polymerization (Fig. 4c).[119] Among these efforts, the most significant insight is to understand the knowledge between prenuclear monomers and functional amorphous states, proclaiming great potential in producing materials with rationally designed amorphous structures and functions.

3.2.1 Nucleation. Nucleation is fundamental in the formation of atoms, ions, or monomers to a new phase, and its ingenious regulation for the precursors in the liquid phase could construct amorphous structure, sequentially producing amorphous materials.[120] For example, in solution synthesis, the ingenious regulation of supersaturation can nucleate the amorphous phase.[121] Additionally, undercooled melt provides a cradle of nucleation in amorphous inorganics, generating liquid metal or alloy to form a solid material with an amorphous structure.[122] This method is used to create metallic glasses, which exhibit unique properties, such as high strength and excellent corrosion resistance.[123] For instance, Fe-Cr-based amorphous alloys significantly enhanced their strength and corrosion resistance after annealing.[124] During the process of amorphization, nucleation appears first, followed by structural relaxation, causing the atomic ordering to increase at short distances and retaining disordered long-term structures.[124,125] The primary focus of structural relaxation is to alleviate residual stress, which results in an increase in activation energy, ΔG^*, leading to a redistribution of chemical elements across the surface. Consequently, the reduction in quenched-in defects leads to a decrease in the number of active sites for corrosion.[124,126] Moreover, some molecular species (*e.g.*, clusters and amorphous nanoparticles) are important for aggregating into dynamically stable amorphous structures.[127] This process contains multiple pathways and is known as ''crystallization by particle attachment'' (CPA) (Fig. 4d).[128] Amorphous phases are the most commonly observed precursors and intermediates in CPA. As part of the biomineralization process, biological vessels facilitate the transfer of amorphous particles and then fuse onto the surface of biominerals to form an amorphous layer.[129] Owing to their moldable nature, amorphous phases can form amorphous layers in the presence of organic matrixes and subsequently undergo shape-preserving crystallization, leading to the generation of minerals.[130] This process reveals the diverse shapes observed in biominerals that occur naturally from the regulation of amorphous phases.

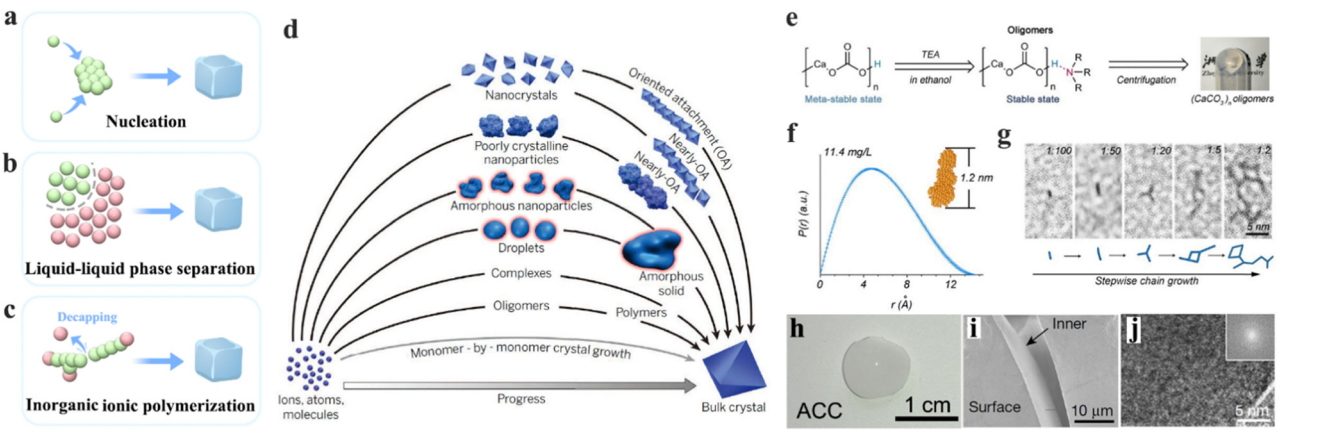

Fig. 4 (a)–(c) Schematic illustration of the representative pathways in the formation of amorphous materials, including nucleation (a), liquid–liquid phase separation (b), and inorganic ionic polymerization. (d) Progress of crystallization from monomers to bulk crystal; red marked are the pathways involved in amorphization. Copyright 2015, AAAS.[128] (e) Schematic illustration of the prosses in the synthesis of the $CaCO_3$ oligomer and its capping effect. (f) Pair distribution of $CaCO_3$ oligomer, inset: corresponding simulated structure. (g) *In situ* observation of the $CaCO_3$ oligomer through a chain growth reaction. (h) Digital photograph of amorphous $CaCO_3$ (ACC) bulk material originating from the $CaCO_3$ oligomer. (i) SEM observation of the surface and inner face of ACC. (j) HRTEM graphs of monolithic ACC, inset: corresponding fast-Fourier-transform image. Copyright 2019, Springer Nature.[119]

Based on nucleation, several synthesis methods have been developed for the construction of amorphous inorganics. Electrodeposition is a representative method for regulating nucleation in fabricating amorphous nanomaterials with controllable kinetics. For instance, Dick and colleagues developed a generalized strategy for preparing amorphous high-entropy metallic glasses through electrosynthesis. This method involved metal salt precursors within water nanodroplets emulsified by dichloroethane.[131] Upon reaction at the electrode, the co-electrodeposition of the metals resulted in the formation of nanoparticles with an amorphous structure.

In addition, researchers have taken advantage of wet-chemical syntheses to prepare amorphous inorganic materials. The commonly used methods include hydrothermal,[132] coprecipitation,[85] and sol–gel methods.[133] Hydrothermal methods have been extensively utilized to manipulate the morphology and composition of nanomaterials. By precisely tuning reaction conditions, such as the choice of metal precursors, surface ligands, reducing agents, and solvents, it is possible to precisely regulate the kinetics and thermodynamics of the nucleation and growth processes of nanocrystals.[134] This manipulation directly impacts the diffusion and migration rate of atoms, enabling the synthesis of amorphous nanomaterials. For instance, Huang *et al.* successfully synthesized porous amorphous $RuTe_2$ nanorods using a straightforward hydrothermal process.[132] Moreover, the coprecipitation method is particularly effective in the production of amorphous metal oxides. For example, Yu *et al.* achieved a wet-chemical method of amorphous NiFeMo oxides within few minutes using a supersaturated coprecipitation strategy. This approach demonstrates the potential for rapid and efficient production of amorphous materials.[85] Moreover, Reiko and colleagues found that the sol–gel method can fabricate amorphous silica through intermediates of silica–lipid hybrid twisted nanoribbons.[134] Accordingly, these methods highlight the exciting pathway offered by wet-chemical methods in synthesizing amorphous inorganic materials and expanding our understanding of the utilization of nucleation.

3.2.2 Liquid–liquid phase separation. Liquid–liquid phase separation is a commonly known phenomenon, widely illustrated by the classic model of oil and water.[135] In the fabrication of amorphous inorganics, this understanding alternatively promotes a pathway, such as an ingenious process to prepare metallic glass and other biominerals. For metallic glasses, non-crystalline alloy systems, such as examples of Nd–Zr–Al–Co, Ni–Nb–Y, Cu–(Zr,Hf)–Al–(Y,Gd), and (Y,Gd)–(Zr,Ti,Hf)–Al–Co, are commonly solidified after the liquid phase separation in nanoscale.[136] In the liquid phase separation, a miscibility gap at low temperatures has advantages in inducing phase separation at small scales, even down to the nanometric scale.[137] Obtaining multicomponent nanostructured phases with well-defined morphologies offers a unique approach to producing both alloy nanoparticles and nanofoams. In biominerals, polymeric stabilizers restrained monomers to assembling aggregations, forming long-range disorder amorphous structures for further bio-utilization.[138] For example, polymer-induced liquid precursor (PILP) is a classical model that can generate an amorphous precursor in the long range and can sequentially induce the generation of an amorphous phase or crystalline.[139] Furthermore, the process of liquid–liquid phase separation can create amorphous nanomaterials with spherical morphology by assembling cluster-based substructures. For example, Yu and his team successfully synthesized stable amorphous calcium carbonate (ACC) nanospheres in a water-deficient ethanol-water binary solution using the gas diffusion method. The ACC nanospheres were formed through a mechanism of liquid–liquid phase separation, rather than the classical nucleation and growth process.[140]

3.2.3 Inorganic ionic polymerization. Inorganic ionic polymerization is a synthesised strategy from the reaction between ionic oligomers, favouriting the fabrication of an amorphous solid.[141–143] Our group provides the first example using calcium carbonate ($CaCO_3$). Typically, stabilized oligomeric $CaCO_3$ clusters were obtained by hydrogen bond-based end-capping (Fig. 4e).[119] Before nucleation, the $CaCO_3$ clusters were typically capped with triethylamine (TEA), consisting of few repeats of $CaCO_3$ molecules and identified as $CaCO_3$ ionic oligomers (Fig. 4f and g). With a rod-like structure and a length of about 1.2 nm, the hydrogen bonds in these clusters could be easily disrupted by evaporating TEA, proclaiming the polymerization and crosslinking processes of the $CaCO_3$ ionic oligomers (Fig. 4h–j). The strategy for ionic oligomer preparation could be extended to more ionic compounds. Accordingly, the ''inorganic ionic polymerization'' process is similar to polymer synthesis, enabling the mouldable construction of various other inorganic ionic compounds.

4. Characterization methodologies

Understanding the atomic structure is significant in characterizing amorphous inorganics, but it is difficult to observe directly because of their disorderliness in the long range. In the early stage, the structure could be illustrated only through statistical methods, which hindered their development. Fortunately, experimental techniques have made great progress in recent decades, presenting an accurate picture of the amorphous structure. More importantly, based on these advanced results, theoretical simulation and calculation ingeniously reveal the cognition of amorphous structures. To address this, representative advanced techniques are introduced.

4.1 Pair distribution function

The pair distribution function (PDF) is widely used to characterize the amorphous structure.[144,145] It describes the possibility as ''*r*'', identifying a specific distance between the central atom and secondary atoms. Generally, functions describing ''*r*'' involve two forms: PDF and radial distribution function (RDF). The PDF calculates the possibility of discovering a second atom at a specific distance from the first, while the RDF describes the

coordinated information, such as distance, number, and angle, in each coordinated shell.[27,146]

(1) Pair distribution function (PDF, $g(r)$): this represents the probability of finding a second atom at a certain distance from the first one (total pairs). The mathematical expression of PDF is

$$g(r) = \rho(r)/\rho_a,$$

where $\rho(r)$ is the atomic number density at distance r from the central atom and ρ_a is the average atomic number density.

(2) Radial distribution function (RDF): this is the probability distribution of finding a second atom at a certain distance r from the first atom (specific pair), which is normalized by the average number density of atoms. The mathematical expression of RDF is

$$\mathrm{RDF}(r) = 4\pi r^2\rho(r),$$

where ρ is the average number density of atoms and $4\pi r^2$ is the surface area of a sphere with radius r.

According to the above structural functions, atomic local details on the neighbour coordination distance of each coordinated shell could be provided by analysing the peak position. It can also reveal the coordination number in each coordination shell by evaluating the integrated area of peaks, and the extent of uncertainty in atomic position stems from disorder by examining the width of the peaks. Simulations and calculations are also helpful in understanding the structures. Simulations, such as the reverse Monte-Carlo method, can fit the RDF results, which would simulate a corresponding atomic structural mode, favouriting chemical calculation and molecular dynamic simulation.

4.2 X-ray and neutron diffraction

Despite the long-range disorder causing amorphous materials to exhibit no diffraction peak in the X-ray diffraction (XRD) pattern, their RDF can be acquired through various techniques by utilizing X-rays or neutron diffraction. The experimental results can be converted through Fourier transformation to acquire PDF and $g(r)$ plots, sequentially structuring the atomic structure *via* reverse Monte Carlo simulations.[147]

Based on analysing neutron diffraction data and utilizing reverse Monte Carlo simulations, Hibble and collaborators proposed a practical three-dimensional chain model to describe the atomic structure of amorphous MoS_3.[148] The research findings reveal that a model comprising chains of MoS_6 octahedra, which share faces and are bonded by disulphides, forming pairs of sulphurs in the shared interfaces, which produces a remarkable correlation with the neutron diffraction data. Additionally, Kerisit and co-workers simulated the atomic structure of amorphous $CaCO_3$ based on X-ray and neutron diffractions (Fig. 5a and b).[149] This work demonstrates that molecular dynamics simulations can understand the atomic location in amorphous structures as well.

The distinction between X-ray and neutron diffraction is obviously determined by their principles of scattering.[150] Specifically, X-ray diffraction uses X-rays, which are a type of

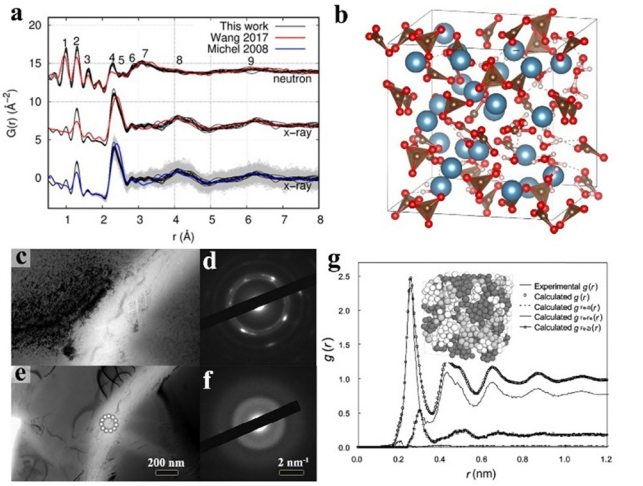

Fig. 5 (a) Pair distribution functions of amorphous $CaCO_3$ in neutron and X-ray diffraction. (b) Structure of amorphous $CaCO_3$ trough molecular simulation. Copyright 2021, American Chemical Society.[149] (c) Microstructure of crystalline $Ti_{59.1}Zr_{37}Cu_{2.3}Fe_{1.6}$ rod after *in situ* heating at 820 K on its advanced amorphous martensite, right side: (d) corresponding crystalline SAED patterns. (e) Microstructure of amorphous $Ti_{59.1}Zr_{37}Cu_{2.3}Fe_{1.6}$ rod before heating, right side: (f) corresponding amorphous SAED patterns. Copyright 2018, Springer Nature.[156] (g) Pair distribution functions of $Fe_{90}Zr_7B_3$ in its experimental and reverse Monte Carlo simulations with total and partial distance distributions, inset: corresponding simulated 3D atomic structure. Copyright 2003, Elsevier.[157]

electromagnetic radiation, to study the structure of materials. The X-rays interact with the atoms in the sample and are scattered in various directions. By analysing the scattered X-rays, researchers can determine the positions of the core atoms and the surrounding atoms with different distances between them. However, neutron diffraction uses neutrons, which are subatomic particles, to study the structure of materials. Neutrons interact differently with atoms than X-rays and can provide additional information on the positions of hydrogen atoms, which are invisible to X-rays.[151] Additionally, neutron diffraction can be used to study materials that are difficult to study using X-rays, such as magnetic materials and materials with low electron density.[152] For amorphous inorganics, both X-ray and neutron diffraction are powerful tools for studying the localized structure at the atomic or molecular level.

4.3 X-ray absorption fine structure analysis

X-ray absorption fine structure (XAFS) is a widely used technique that includes X-ray absorption near edge structure (XANES) and extended X-ray absorption fine structure (EXAFS).[153] It is a prevalent method used to examine the coordination configurations and electronic structures of target atoms through the analyses of element-specific and energy-resolved absorption. The structural analysis is based on the assumption of a short-range order of amorphous phases. In addition to molecular simulation methodology (*e.g.*, reverse Monte Carlo simulation), detailed structural information about amorphous materials can be fitted from experimentally corresponding spectra. For instance, Li and colleagues discovered a decrease in the

coordination number of Ir atoms in amorphous Ir nanosheets compared to their crystalline counterparts through the fitting of Ir L_3-edge EXAFS spectra.[154] Moreover, Ma and his colleagues utilized Fourier-filtered extended EXAFS data and experimental XRD to investigate the short- and medium-range order in amorphous metallic glass.[48] They employed the reverse Monte Carlo simulation technique and *ab initio* molecular dynamics simulation method to determine the nature of these orders. Furthermore, they carried out simulations of the radial distribution function (RDF) at different temperatures while cooling the *ab initio* Ni–P system. These novel experimental and computational techniques allowed them to gain valuable insights into the structure of amorphous metallic glass and its temperature-dependent atomic density.

4.4 Transmission electron microscopy

Transmission electron microscopy (TEM) facilitates the observation of atomic structures, displaying orderly lattice fringes and distinct spots in selected area electron diffraction patterns for crystals.[155] In contrast, the amorphous structure exhibits an intricate maze pattern along with electron diffraction that resembles a corona (Fig. 5d and f).[156] Nonetheless, the emergence of spherical aberration correction technology has led to a resolution enhancement in the sub-angstrom level of TEM. By merging this technology with TEM image simulation, the cognation and direct identification of amorphous structures have been achieved.

The utilization of energy-filtering methods, imaging-plate, and electron energy loss spectroscopy by Hirotsu and his colleagues for electron diffraction PDF analysis (Fig. 5g) of several amorphous alloys presents a deep understanding of their local atomic arrangements and short-range order structures.[157] Moreover, the team employed electron diffraction structure analyses to uncover the atomic structure of amorphous Fe–Zr–B, a key magnetic alloy that generates a soft-magnetic nanostructure upon annealing.[158]

5. Mechanical materials

Amorphous inorganic solids with clearly defined morphology extensively emphasize their mechanical properties because of the distinctiveness of their mechanical attributes, particularly in amorphous metal, metallic oxides, and minerals. These unique properties comprise exceptionally high strength, high hardness, and lower elastic modulus when compared to their corresponding crystalline counterparts. Moreover, mechanical applications integrating amorphous inorganic nanomaterials into hybrid materials are illustrated in this section.

5.1 Amorphous alloy

Amorphization has proven to be an effective method for achieving ultrahigh strength exceeding that of crystalline counterparts.[36] Amorphous alloys are prominent examples of inorganic materials, which are also known as metallic glasses, such as Fe-, Co-, Ni-, and Al-based metallic materials. The mechanics of amorphous alloys have received significant scientific interest owing to their distinctive properties when compared to conventional crystalline metals.[159]

For instance, amorphous alloys can easily adjust to accommodate strain through changes in their atomic neighbourhood owing to their predominant metallic character.[160] At the atomic scale, breaking and reforming of atomic bonds are possible with less concern for the fixed nature of bond angles, as observed in covalent solids, or the balancing of charges, as observed in ionic solids. In contrast to crystalline counterparts, amorphous alloys lack long-range translational symmetry. In crystals, dislocations allow for low-energy or low-stress changes in atomic ranges, whereas rearranging atoms in amorphous alloys is a process that requires relatively high energy or stress levels. For example, the bulk modulus of amorphous alloys is approximately 6% smaller than crystalline counterparts in similar composition.[161] Comparing the two is not always simple because amorphous alloys can crystallize into intricate microstructures with numerous phases. Even when comparing the calculated moduli for an elemental amorphous metal with known crystal values in the simulations, the difference remains consistent.

Furthermore, amorphous alloys are notably different from other categories of engineering materials. Despite having elastic moduli similar to traditional engineering metals, amorphous alloys have substantially superior room-temperature strengths when compared to polycrystals with a similar composition.[162] Although metallic glasses typically exhibit shear localization and brittle failure under normal conditions, there is clear evidence that they can undergo genuine plastic shear flow at a microscopic level.

5.2 Amorphous mineral

In nature, amorphous phases of calcium carbonate or calcium phosphate are commonly used as biomineral fundamentals to build mechanical materials by many organisms, such as crustaceans, fishes, and shells.[163] For example, dragonfish, a kind of deep-sea fish with transparent teeth, constructed an amorphous dentin (Fig. 6a).[164] Their dentin structures are composed of numerous nanometer rods within woven patterns (Fig. 6b and c), featuring an average hardness of 2.1 G $\pm$ 1.2 GPa and a reduced modulus of 16.4 G $\pm$ 7.3 GPa. By comparing the hardness data of white sharks (0.7 G $\pm$ 0.2 GPa) with piranha (0.8 G $\pm$ 0.3 GPa), the dentin of dragonfish is much harder, indicating an outstanding mechanical performance of the amorphous structure.[164] From the perspective of materials, these natural biominerals can provide numerous inspirations for the rational design of biomimetic materials.

With this inspiration, our group utilized amorphous calcium carbonate (ACC) as the foundation for the development of continuous amorphous monolith *via* a pressure-driven particle fusion (Fig. 6d–f).[165] According to the pressure (P) and abundant water (n) related phase diagram, the ''best'' ACC monolith has been fabricated under conditions of P = 3.0 GPa and $n \approx$ 0.3 with a modulus (32.783 $\pm$ 3.537 GPa) and hardness (2.739 GPa $\pm$ 0.249 GPa) (Fig. 6g), which is close to single

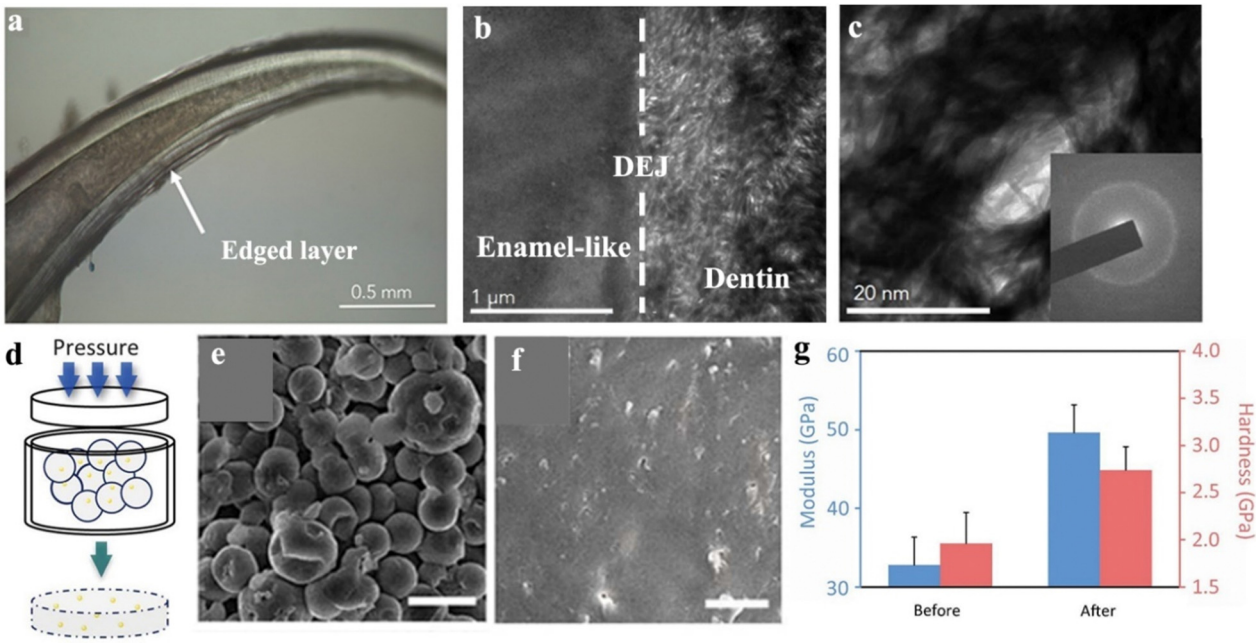

Fig. 6 (a) Microscopic imaging of the concentric layers and hollowness of the tooth of dragonfish. (b) TEM imaging of the dentin-enamel-like junction (DEJ). (c) TEM imaging indicates a woven pattern of dentin structure with numerous nanometer rods (~5 nm diameter), inset: corresponding electron diffraction pattern. Copyright 2019, Elsevier.[164] (d) Schematic illustration of pressure-driven particle fusion progress to obtain an amorphous monolith that originates from amorphous particles. (e) SEM imaging of amorphous $CaCO_3$ particles before particle fusion. (f) SEM imaging of an amorphous $CaCO_3$ monolith formed by particle fusion. (g) Mechanical properties, including modulus and hardness of amorphous $CaCO_3$ monolith before and after optimizing the experimental conditions. Copyright 2021, AAAS.[165]

crystal calcite, and higher than common cement materials. This process leads to the formation of highly resilient and robust structures, and it promotes a moderate synthetic strategy for the application of incompatible thermally sensitive materials.

Moreover, enlightened by the naturally aligned lamellar architecture of nacre, Chen and colleagues created a novel material called amorphous artificial nacre (AAN), performing a biomimetic highly stratified structure (Fig. 7a–d).[166] This was achieved using ultra-thin amorphous alumina nanosheets (AAs) as reinforcing phases with a thickness of approximately 5 nm nm. Through interfacial interactions, the AAs were strongly combined with polylactic acid (PLA), leading to the formation of the unit blocks of the AAN amorphous heterophase (Fig. 7d). The results of the mechanical property tests reveal exceptional toughness (103.5 MJ m^{-3}) of AAN, as well as superior plasticity (500.0%). Moreover, these mechanical results surpass the un-biomimetic structural alumina-reinforced composites and a great count of PLA-based material, indicating the superiorities of the bio-inspired strategy of amorphous inorganic application. This approach enables the development of highly durable and robust structures and provides a feasible synthetic method for mechanical materials *via* the structural biomimicking of amorphous inorganic layers.

In addition, crystallization methods produce traditional inorganic nanoparticles that possess well-ordered crystal structures; however, it may not be conducive to interact between the inorganic particles and organic matrices.[167] Minerals with an amorphous structure have atomic arrangements that lack order, increasing the likelihood of improved ion interactions with organic matrices. For instance, Sun and collaborators produced small amorphous calcium carbonate (ACC) nanoparticles in a polyacrylic acid (PAA) mixture, which resulted in a hydrogel referred to as "mineral plastic".[168] This work indicated that the ACC crosslinked with PAA, resulting in the hydrogel containing nearly half of its weight in mineral content, as well as a feature of being shapable, stretchable, and self-healable. Moreover, Menold and co-workers developed an advancement in "mineral plastic", pushing the development of sustainable, recyclable and cost-effective plastic foam materials.[169]

Amorphous inorganics are more accessible in their regulatable utilization. For instance, the understanding of inorganic ionic oligomers with adjustable molecular weights and crosslinking properties has been a significant development in material design.[141] Through organic–inorganic copolymerization, a polyacrylamide–calcium phosphate oligomer (CPO) with a uniformly structured composition has been synthesized to provide exceptional hardness.[170] Additionally, an amorphous oligomer of calcium phosphate (CaP) has been employed to produce a hybrid mineral (HM).[171] The HM is hierarchically structured bulk material assembled with CaP nanofibers, originating from an amorphous oligomer of calcium phosphate through inorganic ionic polymerization, afterwards enabling plasticity traits to avoid the inherent brittleness of the minerals. Recently, our group reported that calcium carbonate oligomers (CCOs) can

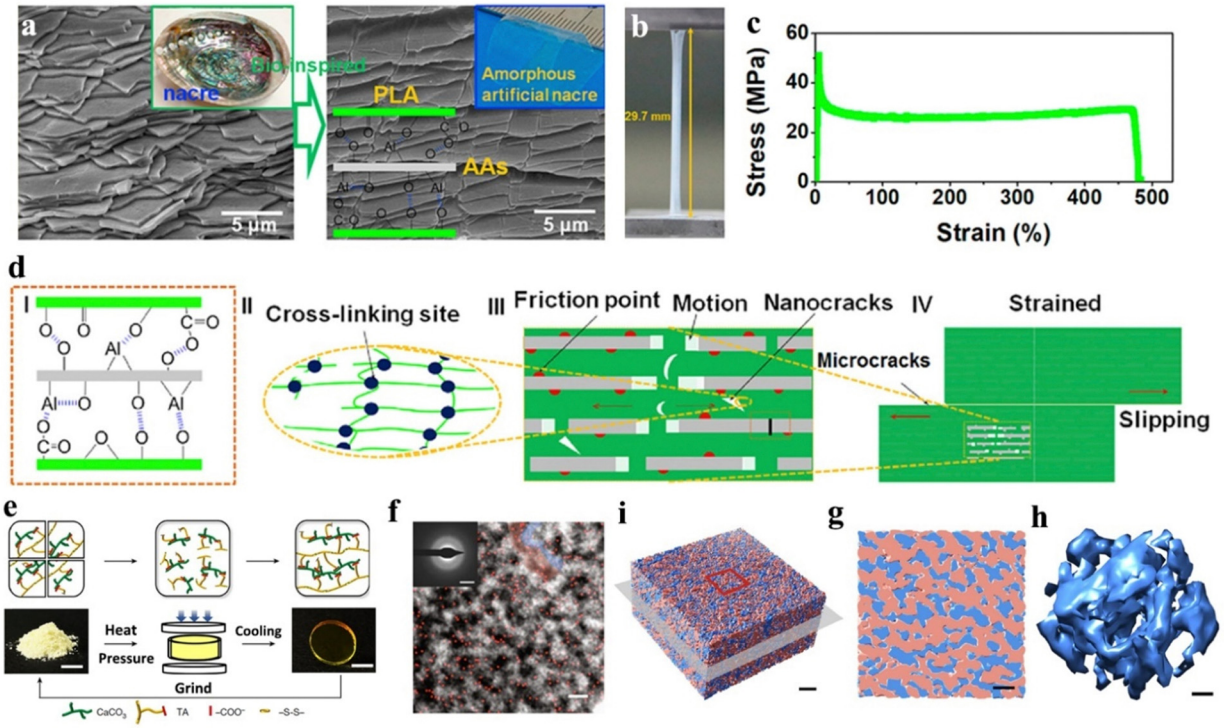

Fig. 7 (a) SEM imaging of natural nacre and amorphous artificial nacre. (b) Digital imaging of straining artificial nacre material. (c) Corresponding straining curve. (d) Schematic illustration of the mechanism in the formation and straining performance of artificial nacre material. Copyright 2019, Elsevier.[166] (e) Displays of the elastic ceramic plastic, namely poly-(TA-CCO) in its formation and structural reversible snapshots. (f) HAADF-STEM imaging of the elastic ceramic plastic, scale bar: 5 nm. Elemental S is distributed as red dots mapping. Inset: Corresponding electron diffraction pattern, scale bar: 3 nm^{-1}. (i) 3D cryo-electron tomography reconstruction of the solid poly-(TA-CCO) with red marked (organic partial poly-TA) and blue marked (inorganic partial $CaCO_3$), scale bar: 5 nm. (g) Magnified display of (i), scale bar: 5 nm. (h) Corresponding 3D $CaCO_3$ network of (i), scale bar: 2 nm. Copyright 2023, Springer Nature.[172]

directly connect with thioctic acid (TA) *via* ionic bonding, thus creating an organic–inorganic hybrid molecule with a formula of $TA_2Ca(CaCO_3)_2$.[172] Under the circumstances of hot-pressing, $TA_2Ca(CaCO_3)_2$ can form an amorphous elastic ceramic plastic (Fig. 7e and f), namely poly-(TA-CCO), with an extraordinary mechanical property that contributes to an inorganic cross-linking from CCO and a polymerization from -S-S- at the TA site. The experimental and computational results show that covalent and ionic networks are homogeneously distributed, leading to an ionic–covalent bi-continuous amorphous structure of the poly-(TA-CCO) (Fig. 7i–h). According to these structural features, poly-(TA-CCO) presents a combined mechanical property of ceramic, rubber, and plastic-like mouldability, which is distinctive in existing mechanical materials. More recently, our group utilized calcium carbonate (CaC) and calcium phosphate (CaP) as a group of oligomers to synthesis an amorphous $Ca(CO_3)_x(PO_4)_{2(1-x)/3}$ ($0 < x < 1$, a-CaCPs) *via* inorganic ionic cocrosslinking. The as-prepared a-CaCPs feature several enhanced mechanical behaviours and provide a regulated potential to form an alloy-like mineral (ALM) after heat-induced synchronous crystallization. The ALMs result in a highly performed inorganic hybrid mineral with a hardness value of 5.6 GPa.[173] As mentioned above, studies have shown that amorphous nanoparticles and newly discovered inorganic ionic oligomers offer superior mechanical improvements. Further understanding of the regulation of amorphous inorganics presents an opportunity to produce materials with enhanced mechanical properties.

6. Electrical materials

The unique electrical properties of amorphous inorganics are distinct from their crystalline counterparts, attracting research interest owing to their intrinsic disordered structure.[174] Notably, amorphous inorganics emphasize great potential for various kinds of electrical devices, such as electrodes, electrolytes, and conductors. Moreover, recent research efforts on amorphous inorganics for advanced electrical materials are illustrated as follows.

6.1 Electrodes

Electrodes are important aspects of many electronic devices, especially batteries, because they are directly involved in electrochemical reactions.[175] For electrode materials, inorganics occupy many quantities in cathode and anode materials. Among these inorganics, most of them are long-term ordering crystalline structures, providing ionic migration paths. For

electrode materials, such as polyanion-type materials, their ingenious crystalline provides a functional structure, but they are limited by their low intrinsic electronic and ionic conductivities, limiting their power performance, which is essential for electrodes.[176] Amorphous inorganics provide an alternative insight into the achievement of disordering structure, which features isotropic ion diffusion routes and many vacant sites, benefiting from fast ion diffusion and providing more ion reaction sites. Accordingly, several represented advances in amorphous are subsequently illustrated, persuading brand-new candidates for electrode application.

6.1.1 Electrodes in lithium-ion batteries. In lithium-ion batteries (LIB), the ingenious design of electrode materials for anode and cathode is a potential strategy to enhance the electrochemical performance of lithium-ion batteries.[177] As the primary part of LIBs, anode materials have attracted increasing attention owing to their direct involvement in electrochemical reactions, sequentially determining their performance *via* their instinct higher capacity.[15] Recently, amorphous inorganics have provided an alternative approach for the enhancement of specific capacity. Because of the regulation of non-crystalline states, several amorphous inorganics, such as SnO_2, TiO_2, and GeO_x, are utilized as high-performed anode materials.[178–180] According to Mou and colleagues, amorphous SnO_2 nanoparticles of exceptionally small sizes exhibit intrinsic isotropy, which can reduce the electrochemical side effects caused by the volume shift of SnO_2 and facilitate the movement of lithium ions through efficient percolation pathways (Fig. 8a).[178] According to the research by Xue and co-workers, amorphous TiO_2 possesses a high capacity for anode materials in lithium-ion batteries (Fig. 8b).[179]

The amorphous TiO_2 offers higher levels of pseudo-capacitance contributions owing to the presence of titanium vacancies and an open framework within their structures

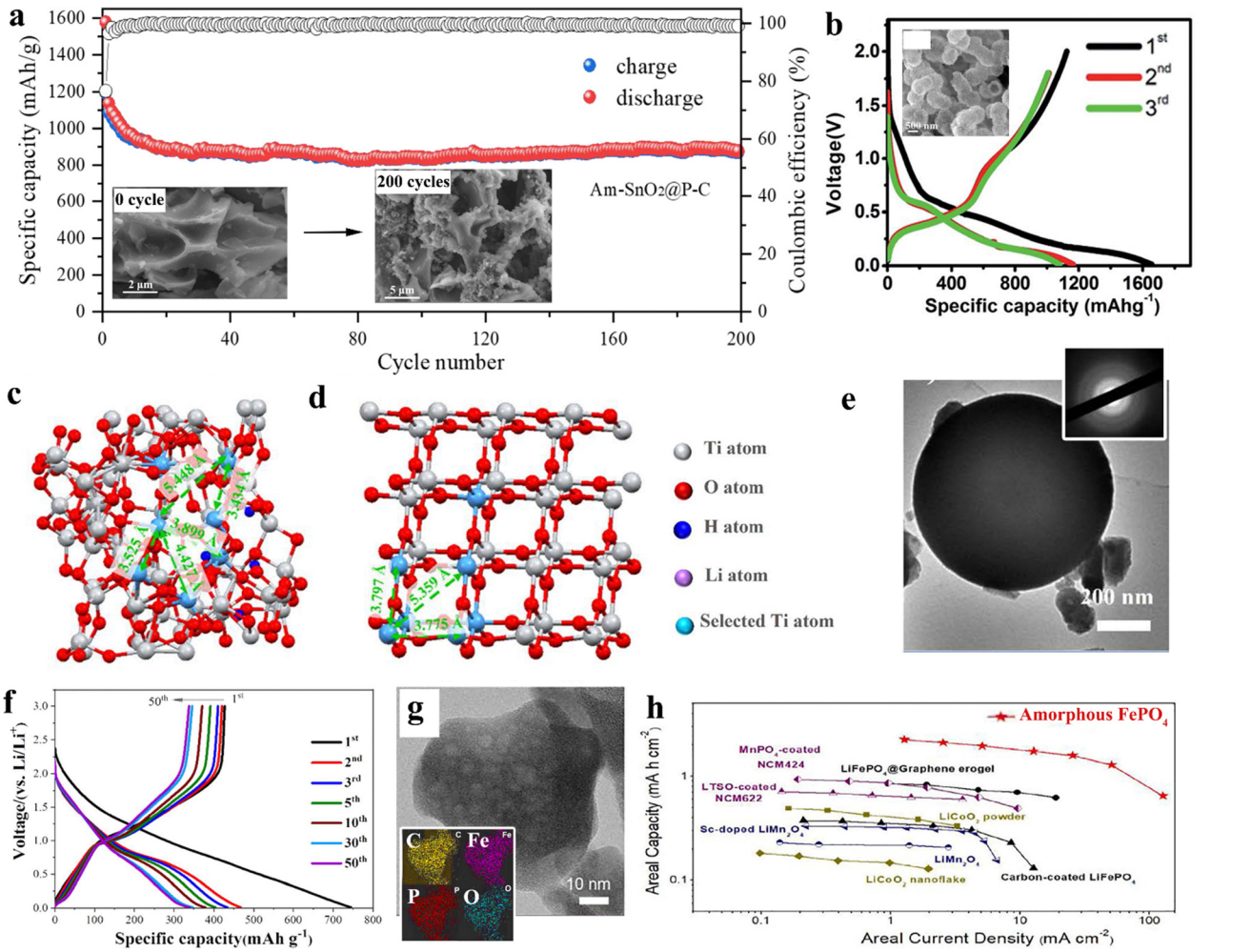

Fig. 8 (a) 200 times cycling charge/discharge performance of amorphous SnO_2, inset corresponding SEM imaging before and 200 times charges. Copyright 2021, Elsevier.[178] (b) Specific capacity of amorphous TiO_2 in 1st, 2nd, and 3rd cycles. (c) and (d) Distinct atomic structure of TiO_2 in its (c) amorphous state and (d) crystalline state. Copyright 2023, Elsevier.[179] (e) TEM of amorphous GeO_x hollow spheres, insert: corresponding electron diffraction. (f) Specific capacity of 50 times cycling of GeO_x hollow spheres. Copyright 2016, The Royal Society of Chemistry.[180] (g) TEM of amorphous $FePO_4$, insert corresponding element mapping. (h) Ashby plots of amorphous $FePO_4$ and other cathode materials in the comparison between areal current density and areal capacity. Reprinted from ref. X with permission from Copyright 2021, Elsevier.[181]

(Fig. 8c and d). Moreover, amorphous GeO_x hollow spheres were prepared by Ma and collaborators, exhibiting exceptional electrochemical performance of amorphous GeO_x hollow spheres attributed to their distinctive porous and hollow nanostructures, as well as their uniform particle size distribution (Fig. 8e and f).[180] This structure not only enhances the specific capacity but also reduces pulverization issues, which lead to particle aggregation, ultimately promoting rate capabilities. As another part of the LIB, cathode materials were also attempted as an alternative through amorphous inorganics. Mo and co-workers illustrated one kind of mesoporous amorphous $FePO_4$ nanoparticles, which exhibited a high reversible capacity, ultra-high-rate capability, and outstanding cycle performance (Fig. 8g and h).[181]

6.1.2 Electrodes in lithium–sulphur batteries. Amorphous inorganics for electrode-related materials have been investigated in recent years. For example, Gueon and co-workers prepared an amorphous titanium suboxide (a-TiO_x) for the promotion of lithium polysulfide (LiPS) adsorption.[182] Compared to crystalline TiO_2, the adsorption of LiPS is approximately 56% higher on the a-TiO_x substrate. This phenomenon contributes to the formation of particulate Li_2S on a-TiO_x, presenting thermodynamically favourable diffusion and clustering at the amorphous surface.

Moreover, alternative insights into the fabrication of a sulphur hybrid amorphous matrix have been investigated in Li–S batteries. Zhou and colleagues prepared one kind of amorphous CoP (a-CoP), structurally interacting with polysulfides with unsaturated Co atoms (Fig. 9a).[183] Abundant active interfaces of a-CoP improved polysulfide transformation, which induces small energy barriers, leading to acceptable volumetric expansion. Consequently, the a-CoP performs excellently in high-rate capability, specific capacity and cycling stability.

6.1.3 Interface in batteries. In recent hybrid solid/liquid battery systems, the fragility of chemistry and electrochemistry at the cathode/electrolyte interface (CEI) has typically been proposed as a research problem. Fortunately, the cathode's surface modification has been demonstrated to be a successful technique for stabilizing the cathode/electrolyte interface and avoiding the development of defective and space-charge layers to a certain extent.[184] By depositing an amorphous CEI layer *in situ* at the interface, the drawbacks of amorphous materials can be significantly overcame owing to their remarkable structure compatibility and flexibility. Liang and colleagues introduced an amorphous CEI buffer layer ($Li_xBO_yF_z$) between Ni-rich cathodes and hybrid electrolytes (Fig. 9b–d). This amorphous CEI layer preserves high compatibility with the surface structure, therefore leading to improved interfacial stability.[185] Simultaneously, the solid/solid interface can effectively reduce the space-charge layer through coordinated chemical potentials, resulting in enhanced interfacial dynamics.

Inspired by ionic polymerization, Dong and co-workers encapsulated the Fe_2O_3 into the amorphous Li_xPO_4 layer. Notably, Li_xPO_4 ionic oligomer cross-linked at Fe_2O_3 to form an amorphous Li_xPO_4 layer through the TEA capping strategy.[186] Compared to other Fe_2O_3-based anode materials, amorphous Li_xPO_4 significantly offers the LIBs many benefits. Although the refined hybrids exceed Li_xPO_4 contents at 5%, they perform a stably reversible capacity ($\sim$1100 mA h g^{-1} at 0.2 A g^{-1}), a high-rate capability ($\sim$615 mA h g^{-1} at 20 A g^{-1}), and a remarkable cycling stability ($\sim$100% after 900 cycles at 0.5 A g^{-1}).

6.2 Conductors

6.2.1 Semiconductors. The design of the amorphous inorganic semiconductors has focused on improving their electrical properties. In the early stage, many studies have revealed that

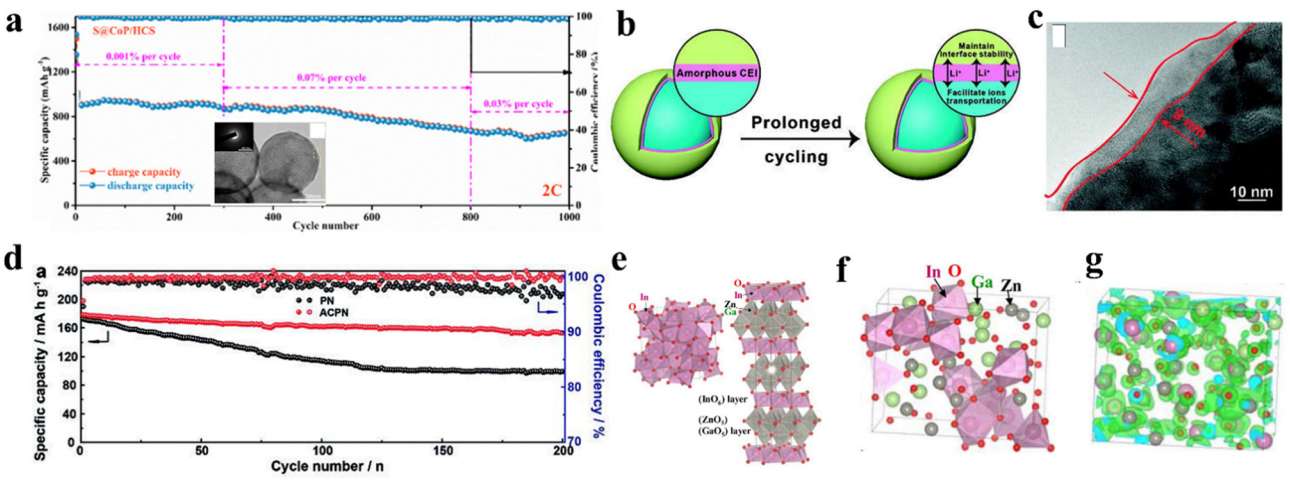

Fig. 9 (a) Long-term cycling charged/discharge performance of the amorphous CoP, inset is the TEM image of the amorphous CoP and corresponding electron diffraction. Copyright 2021, Elsevier.[183] (b) Scheme of amorphous $Li_xBO_yF_z$ layer and its mechanism to facilitate ion transportation. (c) HRTEM of amorphous $Li_xBO_yF_z$ layer. (d) 200 times cycling at 0.5C of amorphous $Li_xBO_yF_z$ layer-modified cathode. Copyright 2020, Wiley VCH.[185] (e) Crystalline structure of InO (left) $InGaZnO_4$ (right), indicating a corner-sharing network structure. (f) Atomic structure of amorphous $InGaZnO_4$ (a-IGZO) indicates an edge-sharing network structure. (g) Green surfaces are conduction band minimum wave functions in a-IGZO. Copyright 2009, Wiley VCH.[189]

amorphous structures cannot afford good electron mobility compared with crystalline counterparts.

For example, the electron mobility of amorphous silicon (a-Si, 2 $cm^2 V^{-1} s^{-1}$) significantly lowers the electron mobility of crystalline silicon (c-Si, 1500 $cm^2 V^{-1} s^{-1}$).[187] On the contrary, amorphous metallic oxide-based materials have caused a semiconductor-revolution since 2000 owing to their superior charge transport properties, also known as carrier mobility with a range of $\mu \sim$ 1–100 $cm^2 V^{-1} s^{-1}$.[188] Compared with crystalline counterparts, amorphous metallic oxides demonstrate higher electron mobilities, which is elucidated by the electronic structure depicted. The ionic nature of oxides plays a significant role in this regard. In the limitation of amorphous silicon, their chemical bonds, consisting of sp^3 or p orbitals, possess strong spatial directivities. In their study on amorphous $InGaZnO_4$ (a-IGZO), Kamiya and colleagues found that the high electron mobility in these materials can be attributed to the contribution of the conduction band minimum, which is primarily composed of spherical *s* orbitals of metal cations (Fig. 9e–g).[189] Compared with crystalline $InGaZnO_4$ (c-IGZO), amorphous structures depicted in Fig. 9g demonstrate that the metal s orbitals of neighbouring atoms largely overlap with one another, forming a conductive network.

6.2.2 Ionic conductors. Solid-state chemists and electrochemists have been striving to develop high-conductivity solid electrolyte materials, as well as known ionic conductors. Amorphous inorganic materials offer an alternative achievement to ionic conductors.[190] According to Lei and his colleagues, amorphous $Na_2Si_2O_5$ serves primarily as a conductor of Na^+ ions, with O_2 and Si^{4+} ions contributing negligibly to ionic conduction. In contrast, the conductivity in crystalline $Na_2Si_2O_5$ functions as an electrical insulator.[191] The preferred route for Na^+ transportation in amorphous $Na_2Si_2O_5$ occurs along the two-dimensional channels created by the SiO_4 tetrahedral layers. The long-range disorder in amorphous $Na_2Si_2O_5$ leads to coulombic attraction between Na and O, promoting the conduction of Na^+ ions.

From this perspective, amorphous inorganics have great potential in electric-relative materials. Compared with their corresponding crystalline counterparts, the instinct orderliness of amorphous structure provides numerous insights for the novel designing of electrodes, such as high-rate capacity and long-term cycling retention. In conductors, the conductivity can be greatly promoted in amorphous oxides (*e.g.*, amorphous $InGaZnO_4$),[189] whereas their corresponding crystalline counterpart exhibits a property of insulation. Therefore, the development and cognation of amorphous inorganics are significant for novel electrical materials.

7. Biomedical materials

The future of biomedical material development is promising because it offers innovative solutions for clinical treatments. To achieve high-performing functional biomedical materials, various efforts are being made, and amorphous inorganics present an alternative approach to fabricating nanomedicines and biominerals. Amorphous inorganics can control the structure and morphology of materials and provide several advantages for bio-functional applications. In this section, we introduce recent findings on amorphous inorganics for their utilization in biomedical materials.

7.1 Nanomedicine

Nanomedicine refers to the utilization of nanotechnology in the field of biomedicine, encompassing drug delivery, therapeutics, and diagnostics. The nanoscale features of nanomedicine introduce several unique advantages, such as a large specific surface area, modifiability, passive accumulation in the tumour through enhanced permeability and retention effect, and prolonged circulation.[43–46] The construction of novel nano- materials has emerged as a highly researched topic at the interdisciplinary frontier of chemistry, material science, and biomedical science. Amorphous inorganic precursors (*e.g.*, nanoparticles and nanophases) possess both nanoscale structural features and potential applications in nanomedicine. This section discusses recent efforts to utilize amorphous structures for effective drug delivery, therapeutics, and diagnosis.

7.1.1 Drug delivery. Amorphous nanostructure presents a large specific surface area and good solubility, acting as an ideal nanocarrier. Amorphous calcium carbonate (ACC), a typically conventional example, has been utilized as a vehicle for drug delivery systems.[192] Wang *et al.* obtained a high aqueous unstable ACC-based advanced nanomedicine using a surface locking/unlocking strategy, employing rapid drug release in cancer cells (Fig. 10a).[193] Moreover, with a modification of physiological fatty acids, a hydrophobic locking shell can be created on the surface of ACC, providing a straightforward path for isolating ACC from the exterior aqueous medium. As fatty acids are favourable for bio-transportation and degradation, ACC-based nanomedicine implemented this feature in drug delivery to enable a locking/unlocking strategy, offering an accessible method to achieve stimulate-responsive drug delivery.[194] Moreover, the instinct feature of pH responsiveness implies that ACC can serve as an ideal drug delivery system, and Xu and colleagues reported one kind of polyacrylic acid–stabilized ACC for pH-responsive drug release to inhibit the tumour.[195]

7.1.2 Therapeutics. As mentioned above, nanosystems are applied as vehicles to deliver pharmic molecules to cure the disease, whereas some amorphous inorganics can directly perform therapeutic efficacy, such as chemotherapy, immunotherapy, and sonotherapy. Liu and co-workers fabricated one kind of amorphous copper iron tellurite nanoparticles (a-CFT NPs), performing catalytic cell-killing efficacy.[196] The amorphous structure allows the tumour to specifically release numerous Cu^+ ions, benefiting from the high-efficiency generation of reactive oxygen species through an intracellular Fenton-like reaction. Moreover, amorphous NiB@IrO_x nanozymes were fabricated by Wang and colleagues, presenting an efficient catalytic reactivity for apoptosis–ferroptosis combination therapy owing to the non-crystallized structure.[45] In addition, Wang

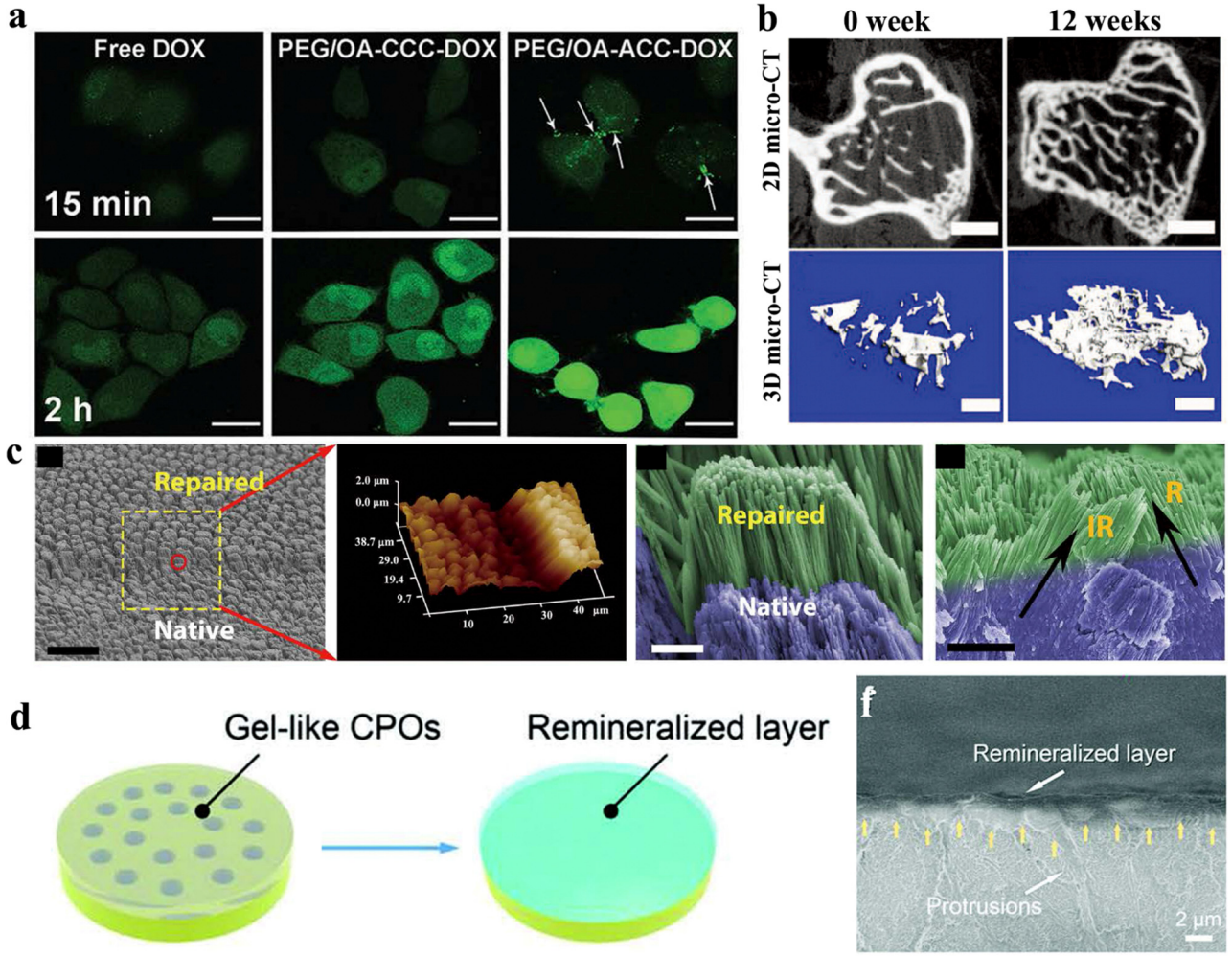

Fig. 10 (a) Confocal imaging of ACC-based nanomedicine in their cellular internalization. Copyright 2017, The Royal Society of Chemistry.[193] (b) 2D and 3D micro-CT photographs of CaP-PILP medicated osteoporotic bone within 0 and 12 weeks. Copyright 2019, Wiley VCH.[46] (c) SEM and AFM images of calcium phosphate ionic oligomers smeared on the surface of native acid-etched enamel and their repairment layer. Copyright 2019, AAAS.[206] (d) Schematic illustration from a gel-like melt to a remineralized layer on the dentin surface with a hybrid composition of calcium phosphate ionic oligomers and collagens. (f) SEM image of the remineralized layer on the surface of the dentin. Copy-right 2022, Wiley-VCH.[44]

and co-workers utilized amorphous calcium carbonate nanoparticles as immunoadjuvants with enabling photosensitizer indocyanine green (ICG), achieving a synergistic photoimmunotherapy for cancer treatment.[197] Li and colleagues prepared amorphous Fe-based nanocluster-coated mesoporous silica nanoagents with ICG loading, synergistic achieving photothermal tumour ablation and oxidative stress amplification.[198] Pariente and co-workers synthesized hybrid nanoparticles that consist of amorphous TiO_2, performing sono-responsive performance for effective cell-killing efficacy of cancer.[21]

7.1.3 Diagnostics. As diagnostics, amorphous inorganics, such as quantum dots, have been investigated in research frontiers for bioactive nanomedical imaging. Compared with nanocrystals, the amorphization of inorganic substances has the potential to alter physical characteristics, such as band gap, absorption coefficient, and refractive index, leading to potential enhancements in imaging performance.[199] Furthermore, amorphous Ag chalcogenide nanoparticles exhibit excellent near-infrared fluorescence, photothermal, and photoacoustic properties. Therefore, Zhao and co-workers provide one kind of $Ag_{2-x}Cu_xS$ quantum dots, namely $Ag_{2-x}Cu_xS$ (a-$Ag_{2-x}Cu_xS$) QDs, which simultaneously integrate tuneable near-infrared fluorophores and enhance photoacoustic imaging capabilities.[200] In this system, Cu doping in amorphous Ag_2S QDs leads to a red-shift of near-infrared fluorescence to the lowest tissue absorption wavelength, which is known as the "first bio-window" (~820 nm). A-$Ag_{2-x}Cu_xS$ QDs exhibited a high photothermal conversion efficiency of 44.0%, benefiting from photothermal and photoacoustic imaging in the bio-window.

7.2 Hard tissue repairment

Hard tissue repairment is recognized as a complex and challenging process. The process begins with the formation of a hematoma (a localized swelling filled with blood) at the site of the injury, which stimulates the recruitment of immune cells

and stem cells. These cells then differentiate into various types of cells, including osteoblasts, which are responsible for the formation of new bone tissue.[201] Over time, osteoblasts lay down new bone tissue, which helps to support and stabilize the broken bone. As the bone continues to heal and regenerate, it eventually becomes strong enough to withstand normal stresses and strains.[202] However, the process of bone repair can be slow and may require medical intervention in some cases, such as in the case of severe fractures or bone injuries. In these cases, surgical intervention or the use of bone grafts or prosthetics may be necessary to aid in the healing and repair processes.

In biomedical materials, the latest advancement utilization for hard tissue engineering presents novel prospects for regenerative therapy. Among various synthetic approaches, amorphous polyphosphates (*e.g.*, calcium phosphate) are considerable inorganic supplements for integration with appropriate bio-active formulations.[203] In biological systems, these integrations can induce the proliferation and differentiation of mesenchymal stem cells, turning a transition to osteogenic or chondrogenic lineages *via* morphogenetic activity.[204] The amorphous phosphates are delivered into the extracellular environments, promoting anabolic processes in bradytrophic tissues, such as cartilage and mineralized bone. Other hard tissue repair materials are polymer-induced liquid precursors (PILPs), which typically consist of charged polymers and ultrasmall-sized inorganic materials (*e.g.*, calcium carbonate or calcium phosphate), and are frequently utilized to mineralize collagen fibers. This material could mimic the natural collagen-HAP crystallization process.[139] However, conventional PILPs are not favourited in the high calcium/phosphorus concentration, leading to poor stability for complete bone repairment. Our group utilized the competitive effects of poly(acrylic acid)–polyaspartic acid (PAA–PASP) to synergistically enhance the stability of ultrahigh concentration and ultrasmall ($\sim$1 nm) calcium phosphate polymer-induced liquid precursor (CaP-PILP) preparations.[46] Although the CaP-PILP produced from this approach had a high viscosity, shear rheological experiments demonstrated its ability to maintain high mobility and a broad linear viscoelastic range. After the injection of CaP-PILP, it was observed that CaP-PILP completely penetrated the interior of the osteoporotic bone model (Fig. 10b). This led to the intramineralization of collagen fibres, which is similar to the natural bone formation processes, resulting in the complete repair of the osteoporotic bone. The biomechanical properties of the bone repaired by CaP-PILP were comparable to those of the natural bone.

Dental caries is a prevalent disease that significantly affects human life by causing erosion and cavitation of tooth tissues, ultimately leading to the loss of tooth tissue. The enamel, which is the hardest biological tissue in the human body, is particularly susceptible to dissolution by acids from food and sugar metabolites. Regrettably, highly mineralized enamel cannot be regenerated in a biological system.[205] Despite attempts by scientists to repair enamel through the use of biomaterials, the complex and well-structured hydroxyapatite formation has made it challenging to duplicate. Recently, our group reported one kind of amorphous precursor, calcium phosphate ionic oligomers, for enamel regenerative application.[206] The study involved the cross-linking of 1.5 $\pm$ 0.3 nm diameter calcium phosphate ionic oligomers on enamel, resulting in the production of an amorphous calcium phosphate (ACP) layer that coated the enamel surface. The integration of ACP with the hydroxyapatite substrate produced an amorphous-crystalline interface similar to that found in the natural biomineral growth process. The hierarchical structure of enamel was successfully reconstructed through an epitaxial growth of hydroxyapatite that occurred spontaneously at the interface of biomimetic saliva (Fig. 10c). This regeneration was attributed to the amorphous–crystalline interface, which was facilitated by cluster-based mineral growth. This regeneration also restored the mechanical strength of the previously damaged enamel.

Afterwards, our group reported a rapid *in situ* crosslinking process of amorphous calcium phosphate oligomers (a-CPOs) on collagen matrices, resulting in proficient reconstruction of organic–inorganic interfaces and producing a biomimetic hybrid repairment of dentin (Fig. 10d and f).[44] Because of the ability of inorganic ionic crosslinking, a-CPOs can be utilized to repair damaged dentin that can rapidly penetrate the dentin matrix, forming a dense and homogeneous calcium phosphate–collagen hybrid in 5 minutes. The resulting organic–inorganic interface fully mimics natural dentin, leading to the full restoration of previously damaged dentin to a healthy state. This approach surpasses the available options in the current dentin treatment.

In addition to amorphous calcium phosphate, another alternative approach for dental repair is the use of amorphous ceramic materials. For instance, Guo and his colleagues experimented with amorphous ZrO_2 as a new repairing agent. This material forms a ceramic layer on damaged enamel under conditions that are tolerable in the oral cavity. The research shows that the resulting ZrO_2 ceramic is amorphous, meaning that it lacks grain boundaries and dislocations. This characteristic gives repaired enamel similar mechanical properties to natural enamel, such as a modulus of approximately 82.5 GPa and a hardness of around 5.2 GPa.[207]

8. Catalytical materials

A long-sought goal of acquiring active catalysts has attracted much attention in the research frontier of chemistry, chemical engineering, and materials science. Inorganic materials preserve great potential for advanced catalytic functions. Among them, amorphous inorganic materials with numerous defects and intrinsic structures have been broadly utilized as chemically active cores of solid catalysts, opening a new avenue for seeking novel catalysts. Compared with their corresponding crystalline counterparts, catalytic capability in amorphous structures demonstrated a superior performance. In this section, a brief introductive illustration is demonstrated, mainly

covering these advanced catalysts for high-performance electrocatalysis and photocatalysis.

8.1 Electrocatalyst

Electrocatalysis offers a sustainable route for producing various substances, but its practical application is hindered by low conversional efficiency.[208] In addition to the chemical composition, recent studies have shown that atoms in nonequilibrium or unsaturated coordinated environments, such as defects, grain boundaries, and interfaces, exhibit enhanced electrocatalytic activity.[24–26,209] To better understand this phenomenon, several concepts have been proposed, including defect engineering, the effects of grain boundaries, and interfacial engineering. The disordered atomic arrangement and its consequent non-equilibrium ligand field considerably influence the electronic structure of the atoms involved, leading to the governed adsorption and desorption of electrocatalytic intermediate products.[209] Based on this mechanism, the concept of amorphous-induced electrocatalytic enhancement (AIEE) is introduced.[210] Combined with AIEE, amorphous inorganics such as metal, alloy, and oxide proceed with advanced electrocatalysis of hydrogen evolution reaction (HER), oxygen evolution reaction (OER),[211] and nitrogen reduction reaction (NRR) are illustrated as follows.

8.1.1 Hydrogen evolution reaction. Hydrogen generation from water splitting has been identified as a crucial source of clean and renewable energy, representing a viable alternative to fossil fuels for sustainable energy usage in the future. Owing to the vacant structure or partially occupied d-orbitals, amorphous metals and alloys exhibit high activity towards the hydrogen evolution reaction (HER).[212] In recent years, the electrocatalytic investigation of amorphous metals and alloys has led to significant advancements in this field. Hydrogen evolution from water splitting is considered an important renewable clean energy source and alternative to fossil fuels for future energy sustainability. Amorphous metal oxide presents an alternative electrocatalytic effect of HER. For instance, amorphous $CoMoO_4$ grown on the Ti substrate (a-$CoMoO_4$/Ti) *via* a two-step hydrothermal route.[213] The a-$CoMoO_4$/Ti achieved an overpotential of 243 mV at 100 mA cm^{-2} in 1 M KOH.

Metallic phosphides are praised as Pt-liked catalysts;[105] meanwhile, their amorphous counterparts exhibit exceeding activity of HER reaction.[214] Owing to their various atomic configurations, amorphous metallic phosphide displayed a different electron structure with numerous defects and unsaturated sites, leading to a smaller Tafel slope. For instance, Zhang and colleagues prepared one kind of amorphous CoP_3 nanowires. Compared with crystalline CoP_3, the amorphous CoP_3 exhibited higher electrocatalytic activities with a smaller Tafel slope of 47 mV dec^{-1}.[215] This is because the binding energies of P $2p_{3/2}$ and Co $2p_{3/2}$ orbits in amorphous CoP_3 shifted with values of 0.8 eV and −0.9 eV, respectively, indicating a less electron transfer between P and Co atoms. Accordingly, the electron transfer ΔG^* of Co was profitably optimized, and the H_2 desorption was promoted, which accelerated HER kinetics thereafter. Furthermore, amorphous NiCoP electrocatalysts, another kind of electrocatalyst, have been extensively investigated to promote HER performance through a bimetallic design. Wu and coworkers found that amorphous $Ni_{0.51}Co_{0.49}P$ is a promising candidate for HER because it exhibits a Tafel slope of 43 mV dec^{-1} in alkaline electrolytes.[216] In general, amorphous metallic phosphides provide insights for amorphous-induced functional enhancement and demonstrate that their performance is related to their regulation in amorphous structures, such as the design of multicomponents.

8.1.2 Oxygen evolution reaction. Compared to crystalline materials, amorphous inorganics are more prone to defects, which can often serve as catalytically active sites playing a critical role in the OER process.[217] Among electrocatalytic OERs, metal oxides are the most extensively studied examples. Amorphous metals also provide outstanding candidates for effective OER. Li and colleagues developed a method for synthesizing numerous amorphous metals and alloy nanosheets with a thickness of less than 10 nm (Fig. 11a–c).[154] Through this approach, they also successfully prepared several other bimetallic and trimetallic nanosheets with a flawless homogeneity of elements, such as the amorphous IrFe

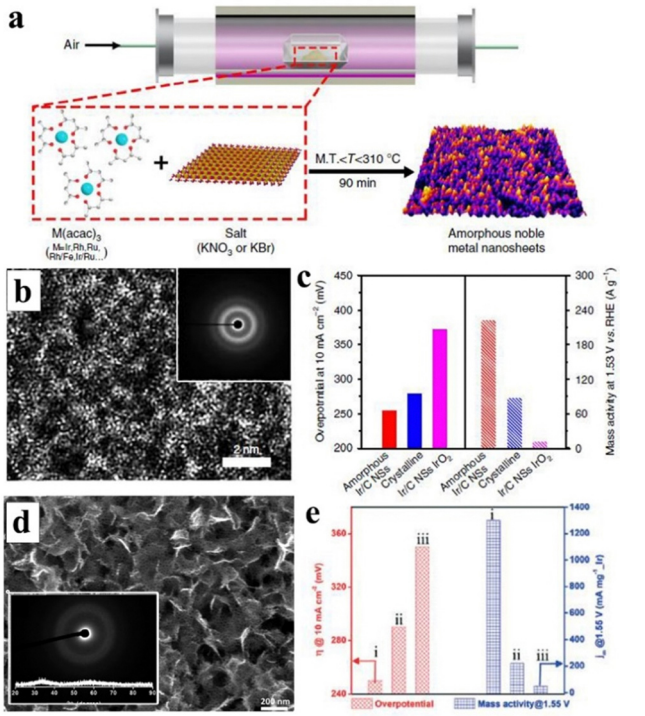

Fig. 11 (a) Schematic illustration of a novel methodology that can generate numerous amorphous metal nanosheets. (b) HETEM image of Ir nanosheets, with inset corresponding to electron diffraction. (c) The left axis side represents the overpotential distribution in different samples at 10 mA cm^{-2}, and the right axis side represents the mass activity at 1.53 V. Copyright 2019, Springer Nature.[154] (d) SEM of IrO_x nanosheets; inset: corresponding electron and X-ray diffraction. (e) Overpotential (left side) at and mass activity at 1.55 V, i-iii represent mesoporous IrO_x@150 °C, mesoporous IrO_2@400 °C and (iii) commercial IrO_2 catalysts, respectively. Copyright 2019, Elsevier.[219]

NSs, RhNi NSs, RuNi NSs, and IrRhRu NSs. Their method presents a simple and effective way of synthesizing amorphous bimetallic NSs. The synthesis of amorphous bimetallic and trimetallic nanosheets offers promising potential for creating exceptional catalysts, such as OER catalysts. Mukherjee and colleagues discovered that the amorphous Ni-Pt alloy outperforms the crystalline alloy, demonstrating the superiority of amorphous materials over their crystalline counterparts in the process of electrocatalysis.[218] Afterwards, they revealed that the mechanism of OER for amorphous Ni–Co alloy in an alkaline solution promotes high overpotential.

Moreover, amorphous oxides and hydroxides have recognized their significant contribution to the OER process. For example, Iridium-based oxides are promising electrocatalysts for OER. Yamachi *et al.* synthesized amorphous IrO_x nanosheets, which demonstrated considerable catalytic activity and stability under both acidic and basic conditions (Fig. 11d and e), rendering them comparable to commercial OER electrocatalysts.[219] The performance of the OER catalyst can be enhanced through the doping of metal elements. The interfacial engineering of composite materials and metals, along with doping, can improve the charge transfer of materials and increase the active site of the interface, ultimately facilitating a more efficient OER catalyst. Liu *et al.* electrodeposited an ultra-fine amorphous FeOOH film onto V-doped NiS NWs using nickel foam as the substrate (eFe/NiVS/NF), exposing numerous active sites and exhibiting robust OER activity.[220]

8.1.3 Nitrogen reduction reaction. NRR is a chemical reaction that aims to produce NH_3 originating from N_2, providing a clean and energy-saving solution in modern society. However, the development to optimize the NH_3 production rate is hindered by the chemical insertion of N_2. In the periodic table, active elements mainly exist as transition metals (d-orbital catalysts), benefiting the reaction of HER or OER, whereas it is difficult to activate the N_2 molecule because of the ultra-low proton and electron affinities of N_2. In contrast, the elements in the main group metals might have catalytic activity because of their distribution of s or p valence electrons, and it is difficult to tune during complex reactions similar to d-orbital catalysts.[221] As the last element of the VA group, Bi ($6s^26p^3$) is hindered in catalytical investigation owing to the hard modulation of oxidation states and the identification of the active phase.[222] To address this issue, Guo and colleagues recently discovered that the amorphization on BiO_x provides a selective electrochemical catalysis for N_2 reduction and NH_3 production. Owing to the amorphization, BiO_x has numerous defects, displaying distinct Bi^{2+} and Bi^{+} oxidation states. These oxidation states fill the 6p orbitals, leading to an improved NRR activity of Bi atoms and partially inhibiting the competing reaction of HER. Thus, compared to d-orbital catalysts, this electrocatalyst performs a totally different behaviour for effective NRR and expands cognition into the design of novel catalysts through amorphized strategy.[65] These ingenious modes for electro-catalytical application proclaim that the amorphization of inorganics can act as candidates for electrocatalysis. The disordered atomic arrangement favours efficient catalysis, whereas their catalytic mechanism still needs more investigation.

8.2 Photocatalyst

Photocatalysis is a highly desirable and environmentally friendly technology that is both sustainable and abundant. The performance of photocatalysis is primarily governed by the topological configuration of the photocatalyst.[23] Thus, a high specific surface area, superior crystallinity, and the presence of heterogeneous facets are vital factors necessary for achieving high photocatalytic efficiency. In contrast to bulk single photocatalysts, amorphous inorganics are high potential photocatalysts owing to their chemical homogeneity.[223] Notably, amorphous structures lack grain boundaries, dislocations, or other imperfections that could induce chemical corrosion. This facilitates the formation of a protective layer that impedes ionic transport, eventually resulting in enhanced corrosion resistance.

A novel microporous amorphous-ZnO@TiO_2 heterostructure was created by Guo and colleagues, featuring outstanding attributes, such as high surface area (336 m^2 g^{-1}), superior mobility of charge carriers, and increased photocatalytic efficiency.[224] In a related work, Bai and colleagues confirmed that amorphous manganese oxides (a-MnO_x) demonstrated superior photoinduced ORR/OER bifunctional catalytic performance compared to crystalline manganese catalysts owing to the high defect state of a-MnO_x with surface-exposed catalytic active sites and abundant edge active sites.[225] Hence, amorphous inorganics are promising materials for utilization in photocatalysis reactions and photoconversion devices.

9. Summary and perspective

In this minireview, we summarized the progress of amorphous inorganics, focusing on their species, atomic structures, typical properties, and applications. Owing to their unique chemical composition and non-crystalline structures, amorphous inorganic materials possess distinctive characteristics, such as strength, specific area, conductivity, and electrochemical capabilities, which present promising potential for various applications in various areas, such as mechanical, electrical, biomedical, and catalytic utilization. Although notable accomplishments have been made in the field of amorphous inorganics, the scope for further development is still a significant task. Our insights and proposed pieces of advice are listed below.

(1) The discovery of seeking more amorphous inorganics is a long-sought goal. The pursuit of more amorphous inorganic materials represents an exciting area of chemistry research with promising applications in a range of fields. The atomically structural difference between amorphous inorganics and their crystalline counterparts exhibits a distinction in their properties. By exploring the unique properties of amorphous inorganics, we can find more opportunities for mechanical, electrical, biomedical, catalytic, and beyond.

(2) The methodologies and techniques used to reveal the radical density function vastly depend on high-energy X-ray and neutron diffraction *via* synchrotron radiation photoelectron spectroscopy, which is difficult to access. In recent advancements, Ag and Mo have been utilized as high-energy X-ray sources to investigate amorphous materials, providing accessibility in the laboratory, yet they still need expansion. Moreover, the equipment that can achieve *in situ* analysis of amorphous materials is considerably necessary. Knowledge of localized changes in amorphization, straining, conductivity, and other spatiotemporal resolutions is still a challenge that requires the development of novel techniques.

(3) Recently, several strategies have promoted brand-new approaches for the construction of amorphous mechanical materials. For instance, the research, which introduced triethylamine (TEA) as the end-capper of ionic oligomers, can stabilize the oligomeric clusters and drive ionic oligomer cross-linking into amorphous solids with controllable synthetic routines from atomic scale to bulk range.[54] For another, amorphous particles can fuse under high pressure, forming an amorphous monolith with a hardness almost exceeding the corresponding single crystal.[95] These findings indicate that various inorganic amorphous solids still need expansion, revealing many possibilities for the preparation of new mechanical materials.

(4) As a typical electrical material, amorphous inorganics demonstrate distinct electrochemical performance compared with their crystalline counterparts. The conductivity of amorphous metallic oxides can be regulated *via* amorphization, favouriting the composed spherical *s* orbitals of metal cations. Moreover, high power density is the evaluated Li^+ ion battery dominated by the performance of cathode materials, whereas commercial products are crystalline electrical materials, such as $LiFePO_4$ and NCM. According to their atomic structure, long-range orderliness may not be a limitation of amorphous cathode materials. The rational design of amorphous electrode materials might pave the way for the development of high-performance batteries.

(5) Concerning biomedical utilization, amorphous inorganics promisingly provide candidates for bone regeneration and dental repairment. However, these hard-tissue repairments are complicated processes hindered by a theoretical understanding of the osteogenesis mechanism. The deep cognation of biomineralization is crucial to investigate, especially in its orderly self-assembly, which has great research value. Furthermore, their impacts need to be refined and optimized by considering their long-term effects on immunity and neuro.

(6) Despite the impressive performance of amorphous inorganics in catalytic applications, their catalytic activity and stability remain unknown because of their intricate atomic and electronic structures. To facilitate the development of high-performed catalysts, the observation of *in situ* characterization technologies and theoretical calculations on amorphous structures should be dedicated to illuminating both the catalytic sites and mechanisms of amorphous nanocatalysts.

Author contributions

R. T. initiated the topic of this review. Z. G., Z. L., and R. T. took part in the writing of this review.

Conflicts of interest

There are no conflicts to declare.

Acknowledgements

The authors acknowledge funding support from the National Natural Science Foundation of China (22022511, 22275161), the National Key Research and Development Program of China (2020YFA0710400) and the Fundamental Research Funds for the Central Universities (226-2022-00022, 2021FZZX001-04).

Notes and references

1 A. Walsh, Inorganic materials: the quest for new functionality, *Nat. Chem.*, 2015, **7**, 274–275.
2 P. H. Gaskell, On the structure of simple inorganic amorphous solids, *J. Phys. C: Solid State Phys.*, 1979, **12**, 4337.
3 T. Egami, T. Iwashita and W. Dmowski, Mechanical Properties of Metallic Glasses, *Metals*, 2013, **3**, 77.
4 Z. Yang, J. Hao and S. P. Lau, Synthesis, properties, and applications of 2D amorphous inorganic materials, *J. Appl. Phys.*, 2020, **127**, 220901.
5 E. V. Sayre and R. W. Smith, Compositional Categories of Ancient Glass, *Science*, 1961, **133**, 1824–1826.
6 V. Rodt, Iron sesquisulfide and the preparation of amorphous iron disulfide, *Angew. Chem.*, 1916, **29**, 422–423.
7 J. Pan, Y. P. Ivanov, W. H. Zhou, Y. Li and A. L. Greer, Strain-hardening and suppression of shear-banding in rejuvenated bulk metallic glass, *Nature*, 2020, **578**, 559–562.
8 D. Ma, A. D. Stoica and X. L. Wang, Power-law scaling and fractal nature of medium-range order in metallic glasses, *Nat. Mater.*, 2009, **8**, 30–34.
9 J.-S. Jung, L. Ren and C. J. O'Connor, Electric, Magnetic, and Photomagnetic Properties of the Amorphous Metallic Spin-Glass $Ni_3(SbTe_3)^2$, *J. Mater. Chem.*, 1992, **2**, 829–832.
10 D. B. Miracle, A structural model for metallic glasses, *Nat. Mater.*, 2004, **3**, 697–702.
11 J. M. Dubois, Properties and applications of quasicrystals and complex metallic alloys, *Chem. Soc. Rev.*, 2012, **41**, 6760–6777.
12 S. Ali Khan, X.-D. Wang, A. Saeed Ahmad, Q.-P. Cao, D.-X. Zhang, Y.-Z. Fang, H. Wang and J.-Z. Jiang, Temperature and Pressure-Induced Polyamorphic Transitions in AuCuSi Alloy, *J. Phys. Chem. C*, 2019, **123**, 20342–20350.
13 M. Mao, C. Yang, Z. Lin, Y. Tong, Q. Zhang, L. Gu, L. Hong, L. Suo, Y. S. Hu, H. Li, X. Huang and L. Chen, Amorphous Redox-Rich Polysulfides for Mg Cathodes, *JACS Au*, 2021, **1**, 1266–1274.

14 J. A. Yuwono, P. Burr, C. Galvin and A. Lennon, Atomistic Insights into Lithium Storage Mechanisms in Anatase, Rutile, and Amorphous TiO_2 Electrodes, *ACS Appl. Mater. Interfaces*, 2021, **13**, 1791–1806.

15 Y. Xin, S. Pan, X. Hu, C. Miao, S. Nie, H. Mou and W. Xiao, Engineering amorphous SnO_2 nanoparticles integrated into porous N-doped carbon matrix as high-performance anode for lithium-ion batteries, *J. Colloid Interface Sci.*, 2023, **639**, 133–144.

16 Z. Tu, G. Yang, H. Song and C. Wang, Amorphous ZnO Quantum Dot/Mesoporous Carbon Bubble Composites for a High-Performance Lithium-Ion Battery Anode, *ACS Appl. Mater. Interfaces*, 2017, **9**, 439–446.

17 J. Troughton and D. Atkinson, Amorphous InGaZnO and metal oxide semiconductor devices: an overview and current status, *J. Phys. Chem. C*, 2019, **7**, 12388–12414.

18 Y. Yu, C. Sun, X. Yin, J. Li, S. Cao, C. Zhang, P. M. Voyles and X. Wang, Metastable Intermediates in Amorphous Titanium Oxide: A Hidden Role Leading to Ultra-Stable Photoanode Protection, *Nano Lett.*, 2018, **18**, 5335–5342.

19 T. He, L. Zu, Y. Zhang, C. Mao, X. Xu, J. Yang and S. Yang, Amorphous Semiconductor Nanowires Created by Site-Specific Heteroatom Substitution with Significantly Enhanced Photoelectrochemical Performance, *ACS Nano*, 2016, **10**, 7882–7891.

20 S. V. Dorozhkin, Synthetic amorphous calcium phosphates (ACPs): preparation, structure, properties, and biomedical applications, *Biomater. Sci.*, 2021, **9**, 7748–7798.

21 A. Pariente, E. Peled, I. Zlotver and A. Sosnik, Hybrid amorphous TiO_2/polymer nanomaterials trigger apoptosis of pediatric cancer cells upon ultrasound irradiation, *Mater. Today Chem.*, 2021, **22**, 100613.

22 Z. Xu, Q. Li, C. Zhang, P. Wang, X. Xu, L. Ran, L. Zhang, G. Tian and G. Zhang, Amorphous ferric oxide-coating selenium core-shell nanoparticles: a self-preservation Pt(IV) platform for multi-modal cancer therapies through hydrogen peroxide depletion-mediated anti-angiogenesis, apoptosis and ferroptosis, *Nanoscale*, 2022, **14**, 11600–11611.

23 S. Sun, P. Song, J. Cui and S. Liang, Amorphous TiO_2 nanostructures: synthesis, fundamental properties and photocatalytic applications, *Catal. Sci. Technol.*, 2019, **9**, 4198–4215.

24 J. Sun, N. Guo, Z. Shao, K. Huang, Y. Li, F. He and Q. Wang, A Facile Strategy to Construct Amorphous Spinel-Based Electrocatalysts with Massive Oxygen Vacancies Using Ionic Liquid Dopant, *Adv. Energy Mater.*, 2018, **8**, 1800980.

25 C. Guo, X. Sun, X. Kuang, L. Gao, M. Zhao, L. Qu, Y. Zhang, D. Wu, X. Ren and Q. Wei, Amorphous Co-doped MoO_x nanospheres with a core–shell structure toward an effective oxygen evolution reaction, *J. Mater. Chem. A*, 2019, **7**, 1005–1012.

26 T. Wu, H. Meng and R. Dang, Amorphous Ta_2O_5-supported Ru as an efficient electrocatalyst for selective hydrogenation of cinnamaldehyde with water as the hydrogen source, *Inorg. Chem. Front.*, 2021, **8**, 4712–4719.

27 X. Han, G. Wu, J. Du, J. Pi, M. Yan and X. Hong, Metal and metal oxide amorphous nanomaterials towards electrochemical applications, *Chem. Commun.*, 2021, **58**, 223–237.

28 S. Hao and D. S. Sholl, Using first-principles calculations to accelerate materials discovery for hydrogen purification membranes by modeling amorphous metals, *Energy Environ. Sci.*, 2008, **1**, 175–183.

29 S. Hao and D. S. Sholl, Rapid prediction of hydrogen permeation through amorphous metal membranes: an efficient computational screening approach, *Energy Environ. Sci.*, 2013, **6**, 232–240.

30 D. M. Tiede, G. Kwon, X. He, K. L. Mulfort and A. B. F. Martinson, Characterizing electronic and atomic structures for amorphous and molecular metal oxide catalysts at functional interfaces by combining soft X-ray spectroscopy and high-energy X-ray scattering, *Nanoscale*, 2020, **12**, 13276–13296.

31 J. Cheng, E. Sivonxay and K. A. Persson, Evaluation of Amorphous Oxide Coatings for High-Voltage Li-Ion Battery Applications Using a First-Principles Framework, *ACS Appl. Mater. Interfaces*, 2020, **12**, 35748–35756.

32 D. Yan, M. Topsakal, S. Selcuk, J. L. Lyons, W. Zhang, Q. Wu, I. Waluyo, E. Stavitski, K. Attenkofer, S. Yoo, M. S. Hybertsen, D. Lu, D. J. Stacchiola and M. Liu, Ultrathin Amorphous Titania on Nanowires: Optimization of Conformal Growth and Elucidation of Atomic-Scale Motifs, *Nano Lett.*, 2019, **19**, 3457–3463.

33 J. Heo, S.-K. Jung, I. Hwang, S.-P. Cho, D. Eum, H. Park, J.-H. Song, S. Yu, K. Oh, G. Kwon, T. Hwang, K.-H. Ko and K. Kang, Amorphous iron fluorosulfate as a high-capacity cathode utilizing combined intercalation and conversion reactions with unexpectedly high reversibility, *Nat. Energy*, 2022, **8**, 30–39.

34 S. M. Clark, B. Colas, D. E. Jacob, J. C. Neuefeind, H. W. Wang, K. L. Page, A. K. Soper, P. I. Schodder, P. Duchstein, B. A. Zubiri, T. Yokosawa, V. Pipich, D. Zahn, E. Spiecker and S. E. Wolf, The nano- and meso-scale structure of amorphous calcium carbonate, *Sci. Rep.*, 2022, **12**, 6870.

35 V. Lacivita, A. S. Westover, A. Kercher, N. D. Phillip, G. Yang, G. Veith, G. Ceder and N. J. Dudney, Resolving the Amorphous Structure of Lithium Phosphorus Oxynitride, *J. Am. Chem. Soc.*, 2018, **140**, 11029–11038.

36 H. Kou, J. Lu and Y. Li, High-strength and high-ductility nanostructured and amorphous metallic materials, *Adv. Mater.*, 2014, **26**, 5518–5524.

37 Y. Hu, D. Schlom, S. Datta and K. Cho, Ilmenite and amorphous $SnTiO_3$ as p-type oxide semiconductors, *J. Mater. Chem. C*, 2023, **11**, 4830–4836.

38 C. Slater, D. Laurencin, V. Burnell, M. E. Smith, L. M. Grover, J. A. Hriljac and A. J. Wright, Enhanced stability and local structure in biologically relevant amorphous materials containing pyrophosphate, *J. Mater. Chem.*, 2011, **21**, 18783.

39 S. J. G. James and D. Martin, Nathalie Fosse, and Lennox Iton, Designing intermediate-range order in amorphous materials, *Nature*, 2002, **419**, 381–384.

40 H. Zhao, F. Li, S. Wang and L. Guo, Wet Chemical Synthesis of Amorphous Nanomaterials with Well-Defined Morphologies, *Acc. Mater. Res.*, 2021, **2**, 804–815.
41 C. Schuh, T. Hufnagel and U. Ramamurty, Mechanical behavior of amorphous alloys, *Acta Mater.*, 2007, **55**, 4067–4109.
42 D. Ding, J. Huang, X. Deng and K. Fu, Recent Advances and Perspectives of Nanostructured Amorphous Alloys in Electrochemical Water Electrolysis, *Energy Fuels*, 2021, **35**, 15472–15488.
43 X. Wang, Y. Zhao, Y. Hu, Y. Fei, Y. Zhao, C. Xue, K. Cai, M. Li and Z. Luo, Activatable Biomineralized Nanoplatform Remodels the Intracellular Environment of Multidrug-Resistant Tumors for Enhanced Ferroptosis/Apoptosis Therapy, *Small*, 2021, **17**, e2102269.
44 L. Yan, C. Zheng, D. Yuan, Z. Guo, Y. Cui, Z. Xie, Z. Chen, R. Tang and Z. Liu, Fast Construction of Biomimetic Organic-Inorganic Interface by Crosslinking of Calcium Phosphate Oligomers: A Strategy for Instant Regeneration of Hard Tissue, *Adv. Healthcare Mater.*, 2022, **11**, e2201161.
45 Q. Wang, F. Shaik, X. Lu, W. Zhang, Y. Wu, H. Qian and W. Zhang, Amorphous NiB@IrO_x nanozymes trigger efficient apoptosis-ferroptosis hybrid therapy, *Acta Biomater.*, 2023, **155**, 575–587.
46 S. Yao, X. Lin, Y. Xu, Y. Chen, P. Qiu, C. Shao, B. Jin, Z. Mu, N. Sommerdijk and R. Tang, Osteoporotic Bone Recovery by a Highly Bone-Inductive Calcium Phosphate Polymer-Induced Liquid-Precursor, *Adv. Sci.*, 2019, **6**, 1900683.
47 D. R. Nelson, Order, frustration, and defects in liquids and glasses, *Phys. Rev. B: Condens. Matter Mater. Phys.*, 1983, **28**, 5515–5535.
48 H. W. Sheng, W. K. Luo, F. M. Alamgir, J. M. Bai and E. Ma, Atomic packing and short-to-medium-range order in metallic glasses, *Nature*, 2006, **439**, 419–425.
49 J. D. Bernal, Geometry of the Structure of Monatomic Liquids, *Nature*, 1960, **185**, 68–70.
50 G. Y. Jung, E. Shin, J. H. Park, B.-Y. Choi, S.-W. Lee and S. K. Kwak, Thermodynamic Control of Amorphous Precursor Phases for Calcium Carbonate *via* Additive Ions, *Chem. Mater.*, 2019, **31**, 7547–7557.
51 S. Grixti, S. Yadav, S. Thorpe and C. Veer Singh, Atomic structure of Ni–Nb–Y amorphous alloys and water-surface adsorption characteristics, *Comput. Mater. Sci.*, 2019, **169**, 109095.
52 Y. Ivanisenko, C. Kübel, S. H. Nandam, C. Wang, X. Mu, O. Adjaoud, K. Albe and H. Hahn, Structure and Properties of Nanoglasses, *Adv. Eng. Mater.*, 2018, **20**, 1800404.
53 K. F. Kelton, G. W. Lee, A. K. Gangopadhyay, R. W. Hyers, T. J. Rathz, J. R. Rogers, M. B. Robinson and D. S. Robinson, First X-ray scattering studies on electrostatically levitated metallic liquids: demonstrated influence of local icosahedral order on the nucleation barrier, *Phys. Rev. Lett.*, 2003, **90**, 195504.
54 Y. Q. Cheng, E. Ma and H. W. Sheng, Atomic level structure in multicomponent bulk metallic glass, *Phys. Rev. Lett.*, 2009, **102**, 245501.
55 W. K. Luo, H. W. Sheng and E. Ma, Pair correlation functions and structural building schemes in amorphous alloys, *Appl. Phys. Lett.*, 2006, **89**, 131927.
56 F. Tavanti, B. Dianat, A. Catellani and A. Calzolari, Hierarchical Short- and Medium-Range Order Structures in Amorphous Ge_xSe_{1-x} for Selectors Applications, *ACS Appl. Electron. Mater.*, 2020, **2**, 2961–2969.
57 T. Egami, How to characterize disorder, *Nucl. Instrum. Meth. B*, 2016, **374**, 2–7.
58 S. Fu, G.-X. Chen, H. Guo, S. Liu, M. Yan, Y. Lou, H. Ying, Z. Yao, Y. Ren, W. Jiang, H. Zhu, H. Hahn, T. Feng and S. Lan, Synthesis of Free-Standing Pd–Ni–P Metallic Glass Nanoparticles with Durable Medium-Range Ordered Structure for Enhanced Electrocatalytic Properties, *Small*, 2023, **19**, 2300721.
59 S. Geiger, O. Kasian, M. Ledendecker, E. Pizzutilo, A. M. Mingers, W. T. Fu, O. Diaz-Morales, Z. Li, T. Oellers, L. Fruchter, A. Ludwig, K. J. J. Mayrhofer, M. T. M. Koper and S. Cherevko, *Nat. Catal.*, 2018, **1**, 508–515.
60 J. Kang, X. Yang, Q. Hu, Z. Cai, L.-M. Liu and L. Guo, Recent Progress of Amorphous Nanomaterials, *Chem. Rev.*, 2023, **123**, 8859–8941.
61 A. C. Y. Liu, E. D. Bøjesen, R. F. Tabor, S. T. Mudie, A. Zaccone, P. Harrowell and T. C. Petersen, Local symmetry predictors of mechanical stability in glasses, *Sci. Adv.*, 2022, **8**, eabn0681.
62 C. A. Schuh, T. C. Hufnagel and U. Ramamurty, Mechanical behavior of amorphous alloys, *Acta Mater.*, 2007, **55**, 4067–4109.
63 H. Zhao, S. Liu, Y. Wei, Y. Yue, M. Gao, Y. Li, X. Zeng, X. Deng, Ni. A. Kotov, L. Guo and L. Jiang, Multiscale engineered artificial tooth enamel, *Science*, 2022, **375**, 551–556.
64 L. Zhou, P. Jiao, L. Fang, L. Liu, Z. Hao, H. Wang, Y.-M. Kang, K. Zhang and J. Chen, Two-Phase Transition Induced Amorphous Metal Phosphides Enabling Rapid, Reversible Alkali-Metal Ion Storage, *ACS Nano*, 2021, **15**, 13486–13494.
65 J. Kang, X. Chen, R. Si, X. Gao, S. Zhang, G. Teobaldi, A. Selloni, L.-M. Liu and L. Guo, Activating Bi p-orbitals in Dispersed Clusters of Amorphous BiO_x for Electrocatalytic Nitrogen Reduction, *Angew. Chem., Int. Ed.*, 2023, **62**, e202217428.
66 S. Ciarella, D. Khomenko, L. Berthier, F. C. Mocanu, D. R. Reichman, C. Scalliet and F. Zamponi, Finding defects in glasses through machine learning, *Nat. Commun.*, 2023, **14**, 4229.
67 X. Yang, R.-Y. Zhang, J. Zhao, Z.-X. Wei, D.-X. Wang, X.-F. Bie, Y. Gao, J. Wang, F. Du and G. Chen, Amorphous Tin-Based Composite Oxide: A High-Rate and Ultralong-Life Sodium-Ion-Storage Material, *Adv. Energy Mater.*, 2018, **8**, 1701827.
68 H. Han, S. Jin, S. Park, Y. Kim, D. Jang, M. H. Seo and W. B. Kim, Plasma-induced oxygen vacancies in amorphous MnO_x boost catalytic performance for electrochemical CO_2 reduction, *Nano Energy*, 2021, **79**, 105492.

69 J. Zhang, R. Yin, Q. Shao, T. Zhu and X. Huang, Oxygen Vacancies in Amorphous InO_x Nanoribbons Enhance CO_2 Adsorption and Activation for CO_2 Electroreduction, *Angew. Chem., Int. Ed.*, 2019, **58**, 5609–5613.

70 Q. Cheng, Z. Yang, Y. Li, J. Wang, J. Wang and G. Zhang, Amorphous/crystalline $Cu_{1.5}Mn_{1.5}O_4$ with rich oxygen vacancies for efficiently photothermocatalytic mineralization of toluene, *Chem. Eng. J.*, 2023, **471**, 144295.

71 Y. Xu, M. Zhou, X. Wang, C. Wang, L. Liang, F. Grote, M. Wu, Y. Mi and Y. Lei, Enhancement of Sodium Ion Battery Performance Enabled by Oxygen Vacancie, *Angew. Chem., Int. Ed.*, 2015, **54**, 8768–8771.

72 Y. Xu, M. Zhou, C. Zhang, C. Wang, L. Liang, Y. Fang, M. Wu, L. Cheng and Y. Lei, Oxygen vacancies: effective strategy to boost sodium storage of amorphous electrode materials, *Nano Energy*, 2017, **38**, 304–312.

73 S. Wen, X. Gu, X. Ding, P. Dai, D. Zhang, L. Li, D. Liu, X. Zhao and J. Yang, Boosting Fast and Stable Alkali Metal Ion Storage by Synergistic Engineering of Oxygen Vacancy and Amorphous Structure, *Adv. Funct. Mater.*, 2022, **32**, 2106751.

74 X. Wang, W. Shi, Z. Jin, W. Huang, J. Lin, G. Ma, S. Li and L. Guo, Remarkable SERS Activity Observed from Amorphous ZnO Nanocages, *Angew. Chem., Int. Ed.*, 2017, **56**, 9851–9855.

75 H. Pan, X. Y. Liu, R. Tang and H. Y. Xu, Mystery of the transformation from amorphous calcium phosphate to hydroxyapatite, *Chem. Commun.*, 2010, **46**, 7415–7417.

76 Y. Cai and R. Tang, Calcium phosphate nanoparticles in biomineralization and biomaterials, *J. Mater. Chem.*, 2008, **18**, 3775–3787.

77 H. Zhao, S. Liu, X. Yang and L. Guo, Role of Inorganic Amorphous Constituents in Highly Mineralized Biomaterials and Their Imitations, *ACS Nano*, 2022, **16**, 17486–17496.

78 J.-S. Lei, Y. Zheng, Y.-F. Meng, F. Wang, Y.-H.-Z. Feng, H.-C. Wang, L.-B. Mao, S.-H. Yu and Z.-L. Wang, Drug Protein-Stabilized Biomimetic Amorphous Mineral Nanoparticles as Superior Drug Carriers, *Adv. Funct. Mater.*, 2022, **32**, 2202928.

79 A. Alhalaweh, C. A. S. Bergström and L. S. Taylor, Compromised in vitro dissolution and membrane transport of multidrug amorphous formulations, *J. Controlled Release*, 2016, **229**, 172–182.

80 X. Yao, L. Yu and G. G. Z. Zhang, Impact of Crystal Nuclei on Dissolution of Amorphous Drugs, *Mol. Pharm.*, 2023, **20**, 1796–1805.

81 Y. Zhou, N. He, Z. Lin, X. Shang, X. Chen, Y. Li, W. Huang, M. Hong, S. Zhao and J. Luo, A Non-π-Conjugated Molecular Crystal with Balanced Second-Harmonic Generation, Bandgap, and Birefringence, *Small*, 2023, 2305473.

82 C. Zhu, X. Mu, J. Popovic, K. Weichert, P. A. V. Aken, Y. Yu and J. Maier, Lithium Potential Variations for Metastable Materials: Case Study of Nanocrystalline and Amorphous $LiFePO_4$, *Nano Lett.*, 2014, **14**, 5342–5349.

83 M. Okubo, E. Hosono, J. Kim, M. Enomoto, N. Kojima, T. Kudo, H. Zhou and I. Honma, Nanosize Effect on High-Rate Li-Ion Intercalation in $LiCoO_2$ Electrode, *J. Am. Chem. Soc.*, 2007, **129**, 7444–7452.

84 Y. Duan, Z.-Y. Yu, S.-J. Hu, X.-S. Zheng, C.-T. Zhang, H.-H. Ding, B.-C. Hu, Q.-Q. Fu, Z.-L. Yu, X. Zheng, J.-F. Zhu, M.-R. Gao and S.-H. Yu, Scaled-Up Synthesis of Amorphous NiFeMo Oxides and Their Rapid Surface Reconstruction for Superior Oxygen Evolution Catalysis, *Angew. Chem., Int. Ed*, 2019, **58**, 15772–15777.

85 J. Liu, J. Nai, T. You, P. An, J. Zhang, G. Ma, X. Niu, C. Liang, S. Yang and L. Guo, The Flexibility of an Amorphous Cobalt Hydroxide Nanomaterial Promotes the Electrocatalysis of Oxygen Evolution Reaction, *Small*, 2018, **14**, 1703514.

86 J. Zhang, Y. Li, Z. Chen, Q. Liu, Q. Chen and M. Chen, Amorphous Electrode: From Synthesis to Electrochemical Energy Storage, *Energy Environ. Mater.*, 2023, **0**, e12573.

87 Z. Lin, M. Mao, C. Yang, Y. Tong, Q. Li, J. Yue, G. Yang, Q. Zhang, L. Hong and X. Yu, Amorphous anion-rich titanium polysulfides for aluminum-ion batteries, *Sci. Adv.*, 2021, **7**, eabg6314.

88 L. Shi, Y. Li, F. Zeng, S. Ran, C. Dong, S.-Y. Leud, S. T. Boles and K. H. Lam, In situ growth of amorphous Fe_2O_3 on 3D interconnected nitrogen-doped carbon nanofibers as high-performance anode materials for sodium-ion batteries, *Chem. Eng. J.*, 2019, **356**, 107–116.

89 J. Kim, D.-H. Seo, H. Kim, I. Park, J.-K. Yoo, S.-K. Jung, Y.-U. Park, W. A. Goddard III and K. Kang, Unexpected discovery of low-cost maricite $NaFePO_4$ as a high-performance electrode for Na-ion batteries, *Energy Environ. Sci.*, 2015, **8**, 540–545.

90 K. Wang, Short-range structure for amorphous intertransition metal alloys, *Nature*, 1979, **278**, 700–704.

91 S. X. Liang, L. C. Zhang, S. Reichenberger and S. Barcikowski, Design and perspective of amorphous metal nanoparticles from laser synthesis and processing, *Phys. Chem. Chem. Phys.*, 2021, **23**, 11121–11154.

92 D. Ma, A. D. Stoica, L. Yang, X. L. Wang, Z. P. Lu, J. Neuefeind, M. J. Kramer, J. W. Richardson and T. Proffen, Nearest-neighbor coordination and chemical ordering in multicomponent bulk metallic glasses, *Appl. Phys. Lett.*, 2007, **90**, 211908.

93 W. Klement Jun, R. H. Willens and P. Duwez, Non-crystalline Structure in Solidified Gold-Silicon Alloys, *Nature*, 1960, **187**, 869–870.

94 Y. Wei, S. Liu, Z. Xiao, H. Zhao, J. Luo, X. Deng and L. Guo, Enamel Repair with Amorphous Ceramics, *Adv. Mater.*, 2020, **32**, 1907067.

95 J. Zhang, E. J. Frankberg, J. Kalikka and A. Kuronen, Room temperature plasticity in amorphous SiO_2 and amorphous Al_2O_3: a computational and topological study, *Acta Mater.*, 2023, **259**, 119223.

96 X. Xu, X. Hu, S. Ren, H. Geng, H. Du and J. Liu, Fine grained Al_2O_3–ZrO_2 (Y_2O_3) ceramics by controlled

crystallization of amorphous phase, *J. Eur. Ceram. Soc.*, 2016, **36**, 1791–1796.

97 W. Ge, P. Zhang, X. Zhang, W. Gao, C. Lu and Y. Ge, Amorphous Alumina: A Bright Red Matrix for Flexible and Transparent Anti-counterfeiting, *ACS Sustainable Chem. Eng.*, 2021, **9**, 10220–10226.

98 C. Zhang, X. Yin, Y. Guo, H. Xie, D. Liu and W. Que, Hole transport free carbon-based high thermal stability $CsPbI_{1.2}Br_{1.8}$ solar cells with an amorphous $InGaZnO_4$ electron transport layer, *Phys. Chem. Chem. Phys.*, 2022, **24**, 18896–18904.

99 M. M. Hasan, Mohit, M. M. Islam, R. N. Bukke, E. Tokumitsu, H.-Y. Chu, S. C. Kim and J. Jang, Improvement of amorphous InGaZnO thin-film transistor with ferroelectric ZrO_x/HfZrO Gate Insulator by 2 step sequential Ar/O_2 treatment, *IEEE Electron. Device Lett.*, 2022, **43**, 725–728.

100 H. Wagner, D. Bedorf, S. Kuchemann, M. Schwabe, B. Zhang, W. Arnold and K. Samwer, Local elastic properties of a metallic glass, *Nat. Mater.*, 2011, **10**, 439–442.

101 C. Zhu, X. Mu, J. Popovic, K. Weichert, P. A. van Aken, Y. Yu and J. Maier, Lithium potential variations for metastable materials: case study of nanocrystalline and amorphous $LiFePO_4$, *Nano Lett.*, 2014, **14**, 5342–5349.

102 E. T. Hwang, R. Tatavarty, J. Chung and M. B. Gu, New functional amorphous calcium phosphate nanocomposites by enzyme-assisted biomineralization, *ACS Appl. Mater. Interfaces*, 2013, **5**, 532–537.

103 L. Chai, S. Liu, S. Pei and C. Wang, Electrodeposited amorphous cobalt-nickel-phosphide-derived films as catalysts for electrochemical overall water splitting, *Chem. Eng. J.*, 2021, **420**, 129686e95.

104 C. C. Weng, J. T. Ren and Z. Y. Yuan, Transition metal phosphidebased materials for efficient electrochemical hydrogen evolution: a critical review, *ChemSusChem*, 2020, **13**, 3357e75.

105 H.-M. Zhang, J.-J. Wang, Y. Meng and J. Sun, Recent advances in amorphous metal phosphide electrocatalysts for hydrogen evolution reaction, *Int. J. Hydrogen Energy*, 2022, **47**, 36084–36097.

106 T. Li, K. Jiang, Y. Li, H. Luo, Z. Wang and Y.-Q. Liu, Crystalline nickel sulfide integrated with amorphous cobalt sulfide as an efficient bifunctional electrocatalyst for water splitting, *Int. J. Hydrogen Energy*, 2023, **48**, 7337–7345.

107 H. Yu, P. Xiao, P. Wang and J. Yu, Amorphous molybdenum sulfide as highly efficient electron-cocatalyst for enhanced photocatalytic H_2 evolution, *Appl. Catal., B*, 2016, **193**, 217–225.

108 C. Chang, L. Wang, L. Xie, W. Zhao, S. Liu, Z. Zhuang, S. Liu, J. Li, X. Liu and Q. Zhao, Amorphous molybdenum sulfide and its Mo–S motifs: structural characteristics, synthetic strategies, and comprehensive applications, *Nano Res.*, 2022, **15**, 8613–8635.

109 H. Kang, Y. Liu, K. Cao, Y. Zhao, L. Jiao, Y. Wang and H. Yuan, Update on anode materials for Na-ion batteries, *J. Mater. Chem. A*, 2015, **3**, 17899–17913.

110 S. Sarkar, S. Roy, Y. Hou, S. Sun, J. Zhang and Y. Zhao, Recent Progress in Amorphous Carbon-Based Materials for Anodes of Sodium-Ion Batteries: Synthesis Strategies, Mechanisms, and Performance, *ChemSusChem*, 2021, **14**, 3693–3723.

111 S. Komaba, W. Murata, T. Ishikawa, N. Yabuuchi, T. Ozeki, T. Nakayama, A. Ogata, K. Gotoh and K. Fujiwara, Electrochemical Na Insertion and Solid Electrolyte Interphase for Hard-Carbon Electrodes and Application to Na-Ion Batteries, *Adv. Funct. Mater.*, 2011, **21**, 3859–3867.

112 E. Johlin, A. Al-Obeidi, G. Nogay, M. Stuckelberger, T. Buonassisi and J. C. Grossman, Nanohole Structuring for Improved Performance of Hydrogenated Amorphous Silicon Photovoltaics, *ACS Appl. Mater. Interfaces*, 2016, **8**(24), 15169–15176.

113 M. C. Wingert, J. Zheng, S. Kwon and R. Chen, Thermal transport in amorphous materials: a review, *Semicond. Sci. Technol.*, 2016, **31**, 113003.

114 M. Xu, D. Shin, P. M. Sberna, R. van der Kolk, A. Cupertino, M. A. Bessa and R. A. Norte, High-Strength Amorphous Silicon Carbide for Nanomechanics, *Adv. Mater.*, 2023, 2306513.

115 J. Xiao and S. Yang, Bio-inspired synthesis: understanding and exploitation of the crystallization process from amorphous precursors, *Nanoscale*, 2012, **4**, 54–65.

116 Z. Ma, B. Li and R. Tang, Biomineralization: Biomimetic Synthesis of Materials and Biomimetic Regulation of Organisms, *Chin. J. Chem.*, 2021, **39**, 2071–2082.

117 H. Wu, Y. Yang, Y. Ou, B. Lu, J. Li, W. Yuan, Y. Wang and Z. Zhang, Early Stage Growth of Rutile Titania Mesocrystals, *Cryst. Growth Des.*, 2018, **18**, 4209–4214.

118 D. Qin, Z. He, P. Li and S. Zhang, Liquid-Liquid Phase Separation in Nucleation Process of Biomineralization, *Front. Chem.*, 2022, **10**, 834503.

119 Z. Liu, C. Shao, B. Jin, Z. Zhang, Y. Zhao, X. Xu and R. Tang, Crosslinking ionic oligomers as conformable precursors to calcium carbonate, *Nature*, 2019, **574**, 394–398.

120 B. Jin, Z. Liu and R. Tang, Recent experimental explorations of non-classical nucleation, *CrystEngComm*, 2020, **22**, 4057–4073.

121 L. O. H. Adam, F. Wallace, A. Fernandez-Martinez, J. D. G. Paolo Raiteri, G. A. Waychunas, S. Whitelam, J. J. D. Y. Jillian and F. Banfield, Microscopic Evidence for Liquid-Liquid Separation in Supersaturated $CaCO_3$ Solutions, *Science*, 2013, **341**, 885–889.

122 W. Song, Y. Wu, H. Wang, X. Liu, H. Chen, Z. Guo and Z. Lu, Microstructural Control *via* Copious Nucleation Manipulated by *In Situ* Formed Nucleants: Large-Sized and Ductile Metallic Glass Composites, *Adv. Mater.*, 2016, **28**, 8156–8161.

123 C. A. C. Souza, D. V. Ribeiro and C. S. Kiminami, Corrosion resistance of Fe-Cr-based amorphous alloys: an overview, *J. Non-Cryst. Solids*, 2016, **442**, 56–66.

124 X. Zhang, Solidification modes and microstructure of Fe–Cr alloys solidified at different undercoolings, *Mater. Sci. Eng., A*, 1998, **247**, 214–221.

125 A. Mikikits-Leitner and B. Sepiol, Mi. Leitner, J. Cieslak, and S. M. Dubiel Nucleation mechanism of the σ-to-α phase transition in $Fe_{1-x}Cr_x$, *Phys. Rev. B: Condens. Matter Mater. Phys.*, 2010, **82**, 100101.

126 F. F. Marzo, A. R. Pierna and M. M. Vega, Effect of irreversible structural relaxation on the electrochemical behavior of $Fe_{78-x}Si_{13}B_9Cr_{(x=3,4,7)}$ amorphous alloys, *J. Non-Cryst. Solids*, 2003, **329**, 108–114.

127 M. Faatz, F. Gröhn and G. Wegner, Amorphous Calcium Carbonate: Synthesis and Potential Intermediate in Biomineralization, *Adv. Mater.*, 2004, **16**, 996–1000.

128 J. J. De Yoreo, P. U. Gilbert, N. A. Sommerdijk, R. L. Penn, S. Whitelam, D. Joester, H. Zhang, J. D. Rimer, A. Navrotsky, J. F. Banfield, A. F. Wallace, F. M. Michel, F. C. Meldrum, H. Colfen and P. M. Dove, CRYSTAL GROWTH. Crystallization by particle attachment in synthetic, biogenic, and geologic environments, *Science*, 2015, **349**, aaa6760.

129 T. Mass, A. J. Giuffre, C. Y. Sun, C. A. Stifler, M. J. Frazier, M. Neder, N. Tamura, C. V. Stan, M. A. Marcus and P. Gilbert, Amorphous calcium carbonate particles form coral skeletons, *Proc. Natl. Acad. Sci. U. S. A.*, 2017, **114**, E7670–E7678.

130 M. W. Glasscott, A. D. Pendergast, S. Goines, A. R. Bishop, A. T. Hoang, C. Renault and J. E. Dick, Electrosynthesis of high-entropy metallic glass nanoparticles for designer, multi-functional electrocatalysis, *Nat. Commun.*, 2019, **10**, 2650.

131 J. Wang, L. Han, B. Huang, Q. Shao, H. L. Xin and X. Huang, Amorphization activated ruthenium-tellurium nanorods for efficient water splitting, *Nat. Commun.*, 2019, **10**, 5692.

132 Y. Okazaki, T. Buffeteau, E. Siurdyban, D. Talaga, N. Ryu, R. Yagi, E. Pouget, M. Takafuji, H. Ihara and R. Oda, Direct Observation of Siloxane Chirality on Twisted and Helical Nanometric Amorphous Silica, *Nano Lett.*, 2016, **16**, 6411–6415.

133 Z. Wu, N. Kumagai and M. Yoshimura, Hydrothermal Formation and Growth of Single- and Double-Layer $BaTiO_3$ and $SrTiO_3$ Films on the Flexible Polymer Film Substrates from Sol–Gel Amorphous Titanium Oxide Films, *Chem. Mater.*, 2000, **12**(11), 3356–3361.

134 A. Navrotsky, Energetic clues to pathways to biomineralization: precursors, clusters, and nanoparticles, *Proc. Natl. Acad. Sci. U. S. A.*, 2004, **101**, 12096–12101.

135 C. D. Keating and R. V. Pappu, Liquid-Liquid Phase Separation: A Widespread and Versatile Way to Organize Aqueous Solutions, *J. Phys. Chem. Lett.*, 2021, **12**, 10994–10995.

136 J. Kim, J. Y. Kim and E. S. Park, Pushing the Boundaries of Multicomponent Alloy Nanostructures: Hybrid Approach of Liquid Phase Separation and Selective Leaching Processes, *Acc. Chem. Res.*, 2022, **55**, 1821–1831.

137 T. Nagase, M. Suzuki and T. Tanaka, Formation of nanoglobules with core–shell structure by liquid phase separation in Fe–Cu–Zr–B immiscible alloy, *J. Alloys Compd.*, 2015, **619**, 332–337.

138 J. S. Evans, "Liquid-like" biomineralization protein assemblies: a key to the regulation of non-classical nucleation, *CrystEngComm*, 2013, **15**, 8377–8588.

139 L. B. Gower, Biomimetic Model Systems for Investigating the Amorphous Precursor Pathway and Its Role in Biomineralization, *Chem. Rev.*, 2008, **108**, 4551–4627.

140 Y.-M. Ju, Y. Zhao, Q.-F. Guan, S.-Y. Yang, W. Wang, B.-B. Yan, Y.-F. Meng, S.-C. Li, P.-P. Tang, L.-B. Mao and S.-H. Yu, Amorphous Calcium Carbonate Cluster Nanospheres in Water-Deficient Organic Solvents, *Angew. Chem., Int. Ed.*, 2022, **61**, e202211254.

141 Y. Sang, K. Qin, R. Tang and Z. Liu, Inorganic ionic polymerization: from biomineralization to materials manufacturing, *Nano Res.*, 2023, DOI: **10.1007/s12274-023-6033-z**.

142 W. F. Fang, L. M. Yan, Z. M. Liu and R. Tang, Revolution in materials science and biomedicine *via* inorganic ionic polymerization (in Chinese), *Sci. Sin. Tech.*, 2023, **53**, 1625–1638.

143 W.-F. Fang, R.-K. Tang and Z.-M. Liu, Polymerization and Crosslinking of Inorganic Ionic Oligomers for Material Construction, *Acta Polym. Sin.*, 2021, **52**(6), 617–633.

144 K. Kodama, S. Iikubo and S.-I. Shamoto, Finite Size Effect of Nanoparticles to the Atomic Pair Distribution Functions, *Acta Crystallogr., Sect. A: Found. Crystallogr.*, 2006, **A62**, 444–453.

145 R. L. McGreevy, Reverse Monte Carlo modelling, *J. Phys.: Condens. Matter*, 2001, **13**, 877–913.

146 A. Hammond and H. Meng, Particle Radial Distribution Function and Relative Velocity Measurement in Turbulence at Small Particle-Pair Separations, *J. Fluid Mech.*, 2021, **921**, A16.

147 R. L. M. D. A. Keen, Structural modelling of glasses using reverse Monte Carlo simulation, *Nature*, 1990, **344**, 423–425.

148 S. J. Hibble and G. B. Wood, Modeling the Structure of Amorphous MoS_3: A Neutron Diffraction and Reverse Monte Carlo Study, *J. Am. Chem. Soc.*, 2004, **126**, 959–965.

149 M. P. Prange, S. T. Mergelsberg and S. N. Kerisit, Ab Initio Molecular Dynamics Simulations of Amorphous Calcium Carbonate: Interpretation of Pair Distribution Function and X-ray Absorption Spectroscopy Data, *Cryst. Growth Des.*, 2021, **21**, 2212–2221.

150 I. M. Gussev, E. C. O'Quinn, M. Tucker, R. C. Ewing, C. Overstreet, J. Neuefeind, M. Everett, Q. Zhang, D. Sprouster, D. Olds, G. Baldinozzi and M. Lang, Systematic study of short- and long-range correlations in RE_3TaO_7 weberite-type compounds by neutron total scattering and X-ray diffraction, *J. Mater. Chem. A*, 2023, **11**, 8886–8903.

151 E. R. Barney, A. C. Hannon, D. Holland, N. Umesaki, M. Tatsumisago, R. G. Orman and S. Feller, Terminal Oxygens in Amorphous TeO_2, *J. Phys. Chem. Lett.*, 2013, **4**, 2312–2316.

152 R. Thapa, C. Ugwumadu, K. Nepal, D. A. Drabold and M. T. M. Shatnawi, Ab initio simulation of amorphous $GeSe_3$ and $GeSe_4$, *J. Non-Cryst. Solids*, 2023, **601**, 121998.

153 J. J. Rehr and R. C. Albers, Theoretical approaches to x-ray absorption fine structure, *Rev. Mod. Phys.*, 2000, **72**, 621–654.
154 G. Wu, X. Zheng, P. Cui, H. Jiang, X. Wang, Y. Qu, W. Chen, Y. Lin, H. Li, X. Han, Y. Hu, P. Liu, Q. Zhang, J. Ge, Y. Yao, R. Sun, Y. Wu, L. Gu, X. Hong and Y. Li, A general synthesis approach for amorphous noble metal nanosheets, *Nat. Commun.*, 2019, **10**, 4855.
155 J. A. Prins, Diffraction of Electrons in Amorphous and in Crystalline Antimony, *Nature*, 1933, **131**, 760–761.
156 L. Zhang, H. Zhang, X. Ren, J. Eckert, Y. Wang, Z. Zhu, T. Gemming and S. Pauly, Amorphous martensite in β-Ti alloys, *Nat. Commun.*, 2018, **9**, 506.
157 Y. Hirotsu, T. Ohkubo, I.-T. Bae and M. Ishimaru, Electron diffraction structure analysis for amorphous materials, *Mater. Chem. Phys.*, 2003, **81**, 360–363.
158 T. Ohkubo, H. Kai and Y. Hirotsu, Structural modeling of Pd–Si and Fe–Zr–B amorphous alloys based on the microphase separation model, *Mater. Sci. Eng.*, 2001, **304–306**, 300–304.
159 J. C. Qiao, Q. Wang, J. M. Pelletier, H. Kato, R. Casalini, D. Crespo, E. Pineda, Y. Yao and Y. Yang, Structural heterogeneities and mechanical behavior of amorphous alloys, *Prog. Mater. Sci.*, 2019, **104**, 250–329.
160 J. Qiao, J. M. Pelletier and R. Casalini, Relaxation of bulk metallic glasses studied by mechanical spectroscopy, *J. Phys. Chem. B*, 2013, **117**, 13658–13666.
161 L. D. S. G. Knuyt and L. M. Stals, Calculation of elastic constants for an amorphous metal and the influence of relaxation, *J. Phys. F: Met. Phys.*, 1986, **16**, 1989–2006.
162 Y. C. Yang, Z. Xia and S. Mukherjee, Unraveling the Structural Statistics and Its Relationship with Mechanical Properties in Metallic Glasses, *Nano Lett.*, 2021, **21**, 9108–9114.
163 A.-W. Xu, Y. Ma and H. Cölfen, Biomimetic mineralization, *J. Mater. Chem.*, 2007, **17**, 415–449.
164 A. Velasco-Hogan, D. D. Deheyn, M. Koch, B. Nothdurft, E. Arzt and M. A. Meyers, On the Nature of the Transparent Teeth of the Deep-Sea Dragonfish, Aristostomias scintillans, *Matter*, 2019, **1**, 235–249.
165 Z. Mu, K. Kong, K. Jiang, H. Dong, X. Xu, Z. Liu and R. Tang, Pressure-driven fusion of amorphous particles into integrated monoliths, *Science*, 2021, **372**, 1466–1470.
166 K. Chen, J. Ding, L. Li, G. Shang, Y. Yue and L. Guo, Amorphous Alumina Nanosheets/Polylactic Acid Artificial Nacre, *Matter*, 2019, **1**, 1385–1398.
167 A. Lotsari, A. K. Rajasekharan, M. Halvarsson and M. Andersson, Transformation of amorphous calcium phosphate to bone-like apatite, *Nat. Commun.*, 2018, **9**, 4170.
168 S. Sun, L. B. Mao, Z. Lei, S. H. Yu and H. Colfen, Hydrogels from Amorphous Calcium Carbonate and Polyacrylic Acid: Bio-Inspired Materials for ''Mineral Plastics'', *Angew. Chem., Int. Ed.*, 2016, **55**, 11765–11769.
169 P. Menold, H. Colfen and C. Stubenrauch, Mineral plastic foams, *Mater. Horiz.*, 2021, **8**, 1222–1229.
170 Y. Yu, Z. Mu, B. Jin, Z. Liu and R. Tang, Organic-Inorganic Copolymerization for a Homogenous Composite without an Interphase Boundary, *Angew. Chem., Int. Ed.*, 2020, **59**, 2071–2075.
171 Y. Yu, Z. Guo, Y. Zhao, K. Kong, H. Pan, X. Xu, R. Tang and Z. Liu, A Flexible and Degradable Hybrid Mineral as a Plastic Substitute, *Adv. Mater.*, 2022, **34**, e2107523.
172 W. Fang, Z. Mu, Y. He, K. Kong, K. Jiang, R. Tang and Z. Liu, Organic–inorganic covalent–ionic molecules for elastic ceramic plastic, *Nature*, 2023, **619**, 293–299.
173 Z. Ma, K. Kong, Y. Yin, Z. Guo, X. Ma, Q. Lin, J. Wang, Y. Shen, X. Lu, X. Xu, X. Kong, Z. Liu and R. Tang, High mechanical strength alloy-like minerals prepared by inorganic ionic cocrosslinking, *Adv. Mater.*, 2024, **36**, 2308017.
174 Q. Gao, M. Gu, A. Nie, F. Mashayek, C. Wang, G. M. Odegard and R. Shahbazian-Yassar, Direct Evidence of Lithium-Induced Atomic Ordering in Amorphous TiO_2 Nanotubes, *Chem. Mater.*, 2014, **26**, 1660–1669.
175 H. Yildirim, J. P. Greeley and S. K. Sankaranarayanan, localized order-disorder transitions induced by Li segregation in amorphous TiO_2 nanoparticles, *ACS Appl. Mater. Interfaces*, 2014, **6**, 18962–18970.
176 Y. Jin, M. Zhang, L. Song and M. Zhang, Research Advances in Amorphous-Crystalline Heterostructures Toward Efficient Electrochemical Applications, *Small*, 2023, **19**, e2206081.
177 T. He, J. Feng, J. Ru, Y. Feng, R. Lian and J. Yang, Constructing Heterointerface of Metal Atomic Layer and Amorphous Anode Material for High-Capacity and Fast Lithium Storage, *ACS Nano*, 2019, **13**, 830–838.
178 H. Mou, Y. Xin, C. Miao, S. Nie, S. Chen and W. Xiao, Amorphous SnO_2 nanoparticles embedded into a three-dimensional porous carbon matrix as high-performance anodes for lithium-ion batteries, *Electrochim. Acta*, 2021, **397**, 139286.
179 C. Xue, Y. Zhang, Z. Nie, C. Du, J. Zhang and J. Zhang, High pseudocapacitive lithium-storage behaviors of amorphous titanium oxides with titanium vacancies and open channels, *Electrochim. Acta*, 2023, **444**, 142021.
180 Q. Ma, M. Ye, P. Zeng, X. Wang, B. Geng and Z. Fang, Size-controllable synthesis of amorphous GeO_x hollow spheres and their lithium-storage electrochemical properties, *RSC Adv.*, 2016, **6**, 15952–15959.
181 R. Mo, D. Rooney, K. Sun and J. N. Wang, 3D holey-graphene frameworks cross-linked with encapsulated mesoporous amorphous $FePO_4$ nanoparticles for high-power lithium-ion batteries, *Chem. Eng. J.*, 2021, **417**, 128475.
182 J. Yang, X. Yang, J. L. Cheong, K. Zaghib, M. L. Trudeau and J. Y. Ying, Nanoboxes with a porous MnO core and amorphous TiO_2 shell as a mediator for lithium–sulfur batteries, *J. Mater. Chem. A*, 2021, **9**, 4952–4961.
183 W. Zhou, D. Zhao, Q. Wu, B. Fan, J. Dan, A. Han, L. Ma, X. Zhang and L. Li, Amorphous CoP nanoparticle composites with nitrogen-doped hollow carbon nanospheres for synergetic anchoring and catalytic conversion

of polysulfides in Li-S batteries, *J. Colloid Interface Sci.*, 2021, **603**, 1–10.

184 J. Cheng, K. D. Fong and K. A. Persson, Materials design principles of amorphous cathode coatings for lithium-ion battery applications, *J. Mater. Chem. A*, 2022, **10**, 22245–22256.

185 J. Y. Liang, X. D. Zhang, X. X. Zeng, M. Yan, Y. X. Yin, S. Xin, W. P. Wang, X. W. Wu, J. L. Shi, L. J. Wan and Y. G. Guo, Enabling a Durable Electrochemical Interface *via* an Artificial Amorphous Cathode Electrolyte Interphase for Hybrid Solid/Liquid Lithium-Metal Batteries, *Angew. Chem., Int. Ed.*, 2020, **59**, 6585–6589.

186 H. Dong, M. Deng, D. Sun, Y. Zhao, H. Liu, M. Xie, W. Dong and F. Huang, Amorphous Lithium-Phosphate-Encapsulated Fe_2O_3 as a High-Rate and Long-Life Anode for Lithium-Ion Batteries, *ACS Appl. Energy Mater*, 2022, **5**, 3463–3470.

187 T. Kamiya and H. Hosono, Material characteristics and applications of transparent amorphous oxide semiconductors, *npg Asia Mater.*, 2010, **2**, 15–22.

188 S.-K. Cha, S. Im, Y.-S. Kim, J. Baeck, J. Noh, K.-S. Park, J. J. Kim and S.-Y. Yoon, Density-Dependent Microstructures and Electromechanical Properties of Amorphous $InGaZnO_4$ Semiconductors: An Ab Initio Study, *ACS Appl. Electron. Mater.*, 2022, **4**, 2545–2551.

189 T. Kamiya, K. Nomura and H. Hosono, Origins of High Mobility and Low Operation Voltage of Amorphous Oxide TFTs: Electronic Structure, Electron Transport, Defects and Doping, *J. Disp. Technol.*, 2009, **5**, 273–288.

190 F. Tian, M. D. Radin and D. J. Siegel, Enhanced Charge Transport in Amorphous Li_2O_2, *Chem. Mater.*, 2014, **26**, 2952–2959.

191 X. Lei, Y. Jee and K. Huang, Amorphous $Na_2Si_2O_5$ as a fast Na^+ conductor: an ab initio molecular dynamics simulation, *J. Mater. Chem. A*, 2015, **3**, 19920–19927.

192 C.-C. Xue, M.-H. Li, Y. Zhao, J. Zhou, Y. Hu, K.-Y. Cai, Y. Zhao, S.-H. Yu and Z. Luo, Tumor microenvironment-activatable Fe-doxorubicin preloaded amorphous $CaCO_3$ nanoformulation triggers ferroptosis in target tumor cells, *Sci. Adv.*, 2020, **6**, eaax1346.

193 C. Wang, X. Liu, S. Chen, F. Hu, J. Sun and H. Yuan, Facile preparation of phospholipid-amorphous calcium carbonate hybrid nanoparticles: toward controllable burst drug release and enhanced tumor penetration, *Chem. Commun.*, 2018, **54**, 13080–13083.

194 C. Wang, S. Chen, Q. Yu, F. Hu and H. Yuan, Taking advantage of the disadvantage: employing the high aqueous instability of amorphous calcium carbonate to realize burst drug release within cancer cells, *J. Mater. Chem. B*, 2017, **5**, 2068–2073.

195 C. Xu, Y. Yan, J. Tan, D. Yang, X. Jia, L. Wang, Y. Xu, S. Cao and S. Sun, Biodegradable Nanoparticles of Polyacrylic Acid–Stabilized Amorphous $CaCO_3$ for Tunable pH-Responsive Drug Delivery and Enhanced Tumor Inhibition, *Adv. Funct. Mater.*, 2019, **29**, 1808146.

196 H. Liu, R. Jiang, Y. Lu, B. Shan, Y. Wen and M. Li, Biodegradable Amorphous Copper Iron Tellurite Promoting the Utilization of Fenton-Like Ions for Efficient Synergistic Cancer Theranostics, *ACS Appl. Mater. Interfaces*, 2022, **14**, 28537–28547.

197 C. Wang, S. Chen, F. Yu, J. Lv, R. Zhao, F. Hu and H. Yuan, Dual-Channel Theranostic System for Quantitative Self-Indication and Low-Temperature Synergistic Therapy of Cancer, *Small*, 2021, **17**, e2007953.

198 J. Li, H. Tian, F. Zhu, S. Jiang, M. He, Y. Li, Q. Luo, W. Sun, X. Liu and P. Wang, Amorphous Ultra-Small Fe-Based Nanocluster Engineered and ICG Loaded Organo-Mesoporous Silica for GSH Depletion and Photothermal-Chemodynamic Synergistic Therapy, *Adv. Healthcare Mater.*, 2022, **11**, e2201986.

199 M. Zhao, H. Zhuang, H. Zhang, B. Li, J. Ming, X. Chen and M. Chen, A LRET Nanoplatform Consisting of Lanthanide and Amorphous Manganese Oxide for NIR-II Luminescence Lifetime Imaging of Tumor Redox Status, *Angew. Chem., Int. Ed*, 2022, **61**, e202209592.

200 Y. Zhao, M. Song, X. Yang, J. Yang, C. Du, G. Wang, J. Yi, G. Shan, D. Li, L. Liu, D. Yan, Y. Li and X. Liu, Amorphous $Ag_{2-x}Cu_xS$ quantum dots: ''all-in-one'' theranostic nanomedicines for near-infrared fluorescence/photoacoustics dual-modal-imaging-guided photothermal therapy, *Chem. Eng. J.*, 2020, **399**, 100613.

201 A. Thiel, M. K. Reumann, A. Boskey, J. Wischmann, R. Eisenhart-Rothe and P. Mayer-Kuckuk1, Osteoblast migration in vertebrate bone, *Biol. Rev.*, 2018, **93**, 350–363.

202 A.-C. Burdus, O. Gherasim, E. Andronescu, B. A. M. Grumezescu and A. Ficai, Inorganic Nanoparticles in Bone Healing Applications, *Pharmaceutics*, 2022, **14**, 770.

203 X. Wang, H. C. Schroder and W. E. G. Muller, Amorphous polyphosphate, a smart bioinspired nano-/bio-material for bone and cartilage regeneration: towards a new paradigm in tissue engineering, *J. Mater. Chem. B*, 2018, **6**, 2385–2412.

204 Y. Y. Hacchou, T. Uematsu, O. Ueda, Y. Usui, S. Uematsu, M. Takahashi, T. Uchihashi, Y. Kawazoe, T. Shiba, S. Kurihara, M. Yamaoka and K. Furusawa, Inorganic polyphosphate: a possible stimulant of bone formation, *J. Dent. Res.*, 2007, **86**, 893–897.

205 Y. Chen, J. Wang, J. Sun, C. Mao, W. Wang, H. Pan, R. Tang and X. Gu, Hierarchical structure and mechanical properties of remineralized dentin, *J. Mech. Behav. Biomed. Mater.*, 2014, **40**, 297–306.

206 C. Shao, B. Jin, Z. Mu, H. Lu, Y. Zhao, Z. Wu, L. Yan, Z. Zhang, Y. Zhou, H. Pan, Z. Liu and R. Tang, Repair of tooth enamel by a biomimetic mineralization frontier ensuring epitaxial growth, *Sci. Adv.*, 2019, **5**, eaaw9569.

207 Y. Wei, S. Liu, Z. Xiao, H. Zhao, J. Luo, X. Deng and L. Guo, Enamel Repair with Amorphous Ceramics, *Adv. Mater.*, 2020, **32**, 1907067.

208 G. Chen, Y. Zhu, H. M. Chen, Z. Hu, S. F. Hung, N. Ma, J. Dai, H. J. Lin, C. T. Chen, W. Zhou and Z. Shao, An Amorphous Nickel-Iron-Based Electrocatalyst

with Unusual Local Structures for Ultrafast Oxygen Evolution Reaction, *Adv. Mater.*, 2019, **31**, e1900883.

209 W. Zhai, T. Sakthivel, F. Chen, C. Du, H. Yu and Z. Dai, Amorphous materials for elementary-gas-involved electrocatalysis: an overview, *Nanoscale*, 2021, **13**, 19783–19811.

210 W. F. Maier, J. A. Martens, S. Klein, J. Heilmann, R. Parton, K. Vercruysse and P. A. Jacobs, Shape-Selective Catalysis with Microporous Amorphous Mixed Oxides, *Angew. Chem., Int. Ed. Engl.*, 1996, **35**, 180–182.

211 Q. Chen, C. Cai, X. Zhang, Q. Zhang, L. Chen, Y. Li, C. Wang and L. Ma, Amorphous FeNi–ZrO_2-Catalyzed Hydrodeoxygenation of Lignin-Derived Phenolic Compounds to Naphthenic Fuel, *ACS Sustainable Chem. Eng.*, 2020, **8**, 9335–9345.

212 P. Li, H. Ni, S. Jiang and H. Wang, Sol–gel preparation of crystalline $Ni_{12}P_5$/N-doped carbon and amorphous Ni–P–C catalysts and their high catalytic performances toward hydrogenation reduction reaction of 4-nitrophenol, *New J. Chem.*, 2021, **45**, 15801–15807.

213 J. Zhao, X. Ren, H. Ma, X. Sun, Y. Zhang, T. Yan, Q. Wei and D. Wu, Synthesis of Self-Supported Amorphous $CoMoO_4$ Nanowire Array for Highly Efficient Hydrogen Evolution Reaction, *ACS Sustainable Chem. Eng.*, 2017, **5**, 10093–10098.

214 Z. Jin, P. Li, X. Huang, G. Zeng, Y. Jin, B. Zheng and D. Xiao, Three-dimensional amorphous tungsten-doped nickel phosphide microsphere as an efficient electrocatalyst for hydrogen evolution, *J. Mater. Chem. A*, 2014, **2**, 18593–18599.

215 J. Zhang, Y. Liu, J. Zhang, Y. Zhang, S. Yuan, D. Wang, J. Lian, Q. Jiang and G. Wang, A self-supporting bifunctional catalyst electrode made of amorphous and porous CoP_3 nanoneedle array: exhaling during overall water splitting, *Electrochim. Acta*, 2021, **393**, 138986e94.

216 J. Yu, Q. Li, Y. Li, C.-Y. Xu, L. Zhen, V. P. Dravid and J. Wu, Ternary Metal Phosphide with Triple-Layered Structure as a Low-Cost and Efficient Electrocatalyst for Bifunctional Water Splitting, *Adv. Funct. Mater.*, 2016, **26**, 7644–7651.

217 M. Risch, K. Klingan, F. Ringleb, P. Chernev, I. Zaharieva, A. Fischer and H. Dau, Water oxidation by electrodeposited cobalt oxides-role of anions and redox-inert cations in structure and function of the amorphous catalyst, *ChemSusChem*, 2012, **5**, 542–549.

218 V. Hasannaeimi, X. Wang, R. Salloom, Z. Xia, J. Schroers and S. Mukherjee, Nanomanufacturing of Non-Noble Amorphous Alloys for Electrocatalysis, *ACS Appl. Energy Mater.*, 2020, **3**, 12099–12107.

219 B. Jiang, J. Kim, Y. Guo, K. C. W. Wu, S. M. Alshehri, T. Ahamad, N. Alhokbany, J. Henzie and Y. Yamachi, Efficient oxygen evolution on mesoporous IrO_x nanosheets, *Catal. Sci. Technol.*, 2019, **9**, 3697–3702.

220 X. Shang, K.-L. Yan, S.-S. Lu, B. Dong, W.-K. Gao, J.-Q. Chi, Z.-Z. Liu, Y.-M. Chai and C.-G. Liu, Controlling electrodeposited ultrathin amorphous Fe hydroxides film on V-doped nickel sulfide nanowires as efficient electrocatalyst for water oxidation, *J. Power Sources*, 2017, **363**, 44–53.

221 Y.-X. Duan, Y.-T. Zhou, Z. Yu, D.-X. Liu, Z. Wen, J.-M. Yan and Q. Jiang, Boosting Production of HCOOH from CO_2 Electroreduction *via* Bi/CeO_x, *Angew. Chem., Int. Ed.*, 2021, **60**, 8798–8802.

222 H. W. Moon and J. Cornella, Bismuth Redox Catalysis: An Emerging Main-Group Platform for Organic Synthesis, *ACS Catal.*, 2022, **12**, 1382–1393.

223 B. R. Goldsmith, B. Peters, J. K. Johnson, B. C. Gates and S. L. Scott, Beyond Ordered Materials: Understanding Catalytic Sites on Amorphous Solids, *ACS Catal.*, 2017, **7**, 7543–7557.

224 S.-Y. Guo, J.-G. Dai, T.-J. Zhao, S.-D. Hou, P. Zhang, P.-G. Wang and G.-X. Sun, A novel microporous amorphous-ZnO@TiO_2/graphene ternary nanocomposite with enhanced photocatalytic activity, *RSC Adv.*, 2017, **7**, 36787–36792.

225 F. Bai, Y. He, L. Xu, Y. Wang, Y. Wang, Z. Hao and F. Li, Improved ORR/OER bifunctional catalytic performance of amorphous manganese oxides prepared by photochemical metal-organic deposition, *RSC Adv.*, 2022, **12**, 2408–2415.

